Available online at www.sciencedirect.com

SCIENCE DIRECT®

Remote Sensing of Environment 99 (2005) 187 – 219

Remote Sensing of Environment

www.elsevier.com/locate/rse

Multispectral imaging contributions to global land ice measurements from space

Jeffrey S. Kargel [a,*], Michael J. Abrams [b], Michael P. Bishop [c], Andrew Bush [d], Gordon Hamilton [e], Hester Jiskoot [f], Andreas Kääb [g], Hugh H. Kieffer [h], Ella M. Lee [a], Frank Paul [g], Frank Rau [i], Bruce Raup [j], John F. Shroder [c], Deborah Soltesz [a], David Stainforth [k], Leigh Stearns [e], Rick Wessels [l]

[a] *University of Arizona, Tucson, AZ 85721, USA*
[b] *Jet Propulsion Laboratory, Pasadena, CA, USA*
[c] *University of Nebraska at Omaha, Omaha, NE, USA*
[d] *Department of Earth and Atmospheric Sciences, University of Alberta, Edmonton, Alberta, Canada T6G 2E3*
[e] *Climate Change Institute, University of Maine, USA*
[f] *Department of Geography, University of Lethbridge, AB, Canada*
[g] *Department of Geography, Glaciology and Geomorphodynamics Group, University of Zurich, Winterthurerstr. 190, CH-8057 Zurich, Switzerland*
[h] *Celestial Reasonings, Carson City, NV, USA, and U.S. Geol. Survey (Emeritus)*
[i] *Inst. Physische Geographie, University of Freiburg, Germany*
[j] *National Snow and Ice Data Center, University of Colorado, 449 UCB, Boulder, CO 80309, USA*
[k] *Oxford University, Oxford, England*
[l] *Alaska Volcano Observatory, U.S. Geological Survey, Anchorage, Alaska, USA*

Received 8 March 2005; received in revised form 30 June 2005; accepted 5 July 2005

Abstract

Global Land Ice Measurements from Space (GLIMS) is an international consortium established to acquire satellite images of the world's glaciers, analyse them for glacier extent and changes, and assess change data for causes and implications for people and the environment. Although GLIMS is making use of multiple remote-sensing systems, ASTER (Advanced Spaceborne Thermal Emission and reflection Radiometer) is optimized for many needed observations, including mapping of glacier boundaries and material facies, and tracking of surface dynamics, such as flow vector fields and supraglacial lake development. Software development by GLIMS is geared toward mapping clean-ice and debris-covered glaciers; terrain classification emphasizing snow, ice, water, and admixtures of ice with rock debris; multitemporal change analysis; visualization of images and derived data; and interpretation and archiving of derived data. A global glacier database has been designed at the National Snow and Ice Data Center (NSIDC, Boulder, Colorado); parameters are compatible with and expanded from those of the World Glacier Inventory (WGI). These technology efforts are summarized here, but will be presented in detail elsewhere. Our presentation here pertains to one broad question: How can ASTER and other satellite multispectral data be used to map, monitor, and characterize the state and dynamics of glaciers and to understand their responses to 20th and 21st century climate change? Our sampled results are not yet glaciologically or climatically representative. Our early results, while indicating complexity, are generally consistent with the glaciology community's conclusion that climate change is spurring glacier responses around the world (mainly retreat). Whether individual glaciers are advancing or retreating, the aggregate average of glacier change must be climatic in origin, as nonclimatic variations average out. We have discerned regional spatial patterns in glaciological response behavior; these patterns are best attributed to climate-change variability and to regional differences in glacier size and response times. In many cases, glacier length changes under-represent the magnitude of glacier ablation, because thinning (sometimes without immediate length changes) is also important. An expanded systematic, uniform analysis of many more glaciers is needed to isolate the glacier response components due to climatic and nonclimatic perturbations, to produce quantitative measures of regional variation in glacier changes, and to predict future regional glacier trends relevant to water

* Corresponding author.
E-mail address: kargel@hwr.arizona.edu (J.S. Kargel).

0034-4257/$ - see front matter
doi:10.1016/j.rse.2005.07.004

resources, glaciological hazards, and global sea level. This comprehensive assessment (to be completed in stages) is expected to lend a critically needed filter to identify successful climate models that explain recent glacier changes and change patterns (and hence, are apt to describe future changes) and to eliminate unsuccessful models.

Keywords: ASTER; Glacier monitoring; Cryosphere; GLIMS; Glacier Land Ice Measurements from Space

1. Introduction

Glacier retreat is widespread; there have been many recent disappearances of small glaciers (Dyurgerov & Meier, 1997; Haeberli & Beniston, 1998; Hastenrath & Ames, 1995; Kaser et al., 1990). Even the fate of polar ice sheets is uncertain (Bindschadler & Bentley, 2002; Oppenheimer, 1998; Rignot et al., 2004). Glacier monitoring is justified by the significance of glaciers for: (1) glacial hazards (Kääb et al., 2002; Yamada & Sharma, 1993); (2) water resources (Fukushima et al., 1991; Hewitt, 1961; Shiyin et al., 2003; Yamada & Motoyama, 1988; Yang & Hu, 1992); (3) climate change (Haeberli & Beniston, 1998; Mayewski et al., 1980; Oerlemans, 1994); and (4) sea-level rise (Church et al., 2001; Gregory & Oerlemans, 1998; Warrick et al., 1996) (Fig. 1). Thus, we have utilized ASTER (Advanced Spaceborne Thermal Emission and reflection Radiometer) and other satellite remote-sensing systems to study glacier state and dynamics.

There is no longer any reasonable doubt about why the aggregate of glaciers is exhibiting profound changes: global climate of the 20th century changed at an average rate beyond combined uncertainties and at a magnitude unprecedented in all the last millennium (Albritton et al., 2001). The primary cause of climate change is recognized to be rising levels of atmospheric carbon dioxide and other greenhouse gases (Cubasch et al., 2001). Global atmospheric CO_2 concentrations have risen by 3% (relative), and a far more potent trace greenhouse gas, HFC-23, has risen by about 40% (relative), just between ASTER's launch (Dec. 1999) and final submission of this paper (June 2005). Most of these gases are being emitted at increasing rates (Albritton et al., 2001); inevitably, climate and glaciers will change at accelerating rates in the future.

The typical magnitude of glacier retreat experienced in the last 100 years and likely in the next 50 years can be understood by the following simple calculation. About 1 K warming has occurred over most glacierized areas in the last 100 years; the same magnitude warming is expected over the next 50 years. For a typical adiabatic gradient of 8 K/km, and ignoring any attendant changes in precipitation (which may be a positive or negative increment as warming proceeds), the glacial equilibrium-line altitude (ELA, where annual snow accumulation balances ablation) would rise by roughly 125 m; for glacier longitudinal surface slopes typically ranging from 4% (for valley glaciers) to 40% (for cirque glaciers), the ELA would thus recede up-valley by around 300 m longitudinally (for cirque glaciers) to 3000 m (for valley glaciers) in the absence of attendant precipitation changes. Terminus positions may change by comparable or larger amounts. Except for glaciers exhibiting special dynamical mechanisms, these are the right orders of magnitude of changes commonly observed in the last century.

The glacier cases shown here were chosen to highlight a complexity to glacier change; this complexity is best explained as due to a combination of heterogeneous climate changes and individualized glacier attributes, environments, and processes. We defer strong conclusions about specific glacier process/environment/response relationships until we have made a comprehensive, uniform glacier-change assessment, which will finally resolve many remaining uncertainties of concern to glaciologists and climatologists. A large digital inventory of glacier-state and change data is the goal of our project, GLIMS (Global Land Ice Measurements from Space; http://www.glims.org); this inventory will enable the tackling of big questions regarding future glacier hydrology and global climate (Fig. 1).

Statistical approaches have been applied to global glacier aggregates (Haeberli et al., 1999; Oerlemans, 1994) from mainly field data sources utilizing fairly small numbers of glaciers. A recent global dominance of negative glacier mass balance has been established (Bahr, 1997a,b; Haeberli et al., 1999; Oerlemans, 1994). Statistical analysis can relate changes in simple parameters, such as glacier area or length, to volume and net annual mass balance (Bahr, 1997a,b; Meier & Bahr, 1996), which conventionally is computed from field data. Oerlemans used glacier variations to back-compute global warming rates. Different individual glaciers and regions of glaciers are exhibiting different responses, but the ensemble of glacier variations indicates rapid loss of ice mass despite increasing average snow accumulation (Dyurgerov & Meier, 2000).

Fig. 1. The "who" and "why" of GLIMS (Global Land Ice Measurements from Space). (A) GLIMS organization, areas of detailed GLIMS database entries, figure locations, and a few climatological and oceanographic elements which strongly affect or are influenced by glaciation and which shift in position or intensity as global warming proceeds. (B) Diagrammatic justification for world glacier monitoring. Center of the diagram illustrates key elements of basic glaciological science; yellow-green elements are key areas of investigation by GLIMS. Stream flow and glacier net mass balance (shown in purple in the "science" part of the diagram) are the key links between glaciers and their practical importance to people and natural ecosystems and our understanding of climate change, as shown in the "Impacts" and "Fundamental Understanding" parts of the diagram.

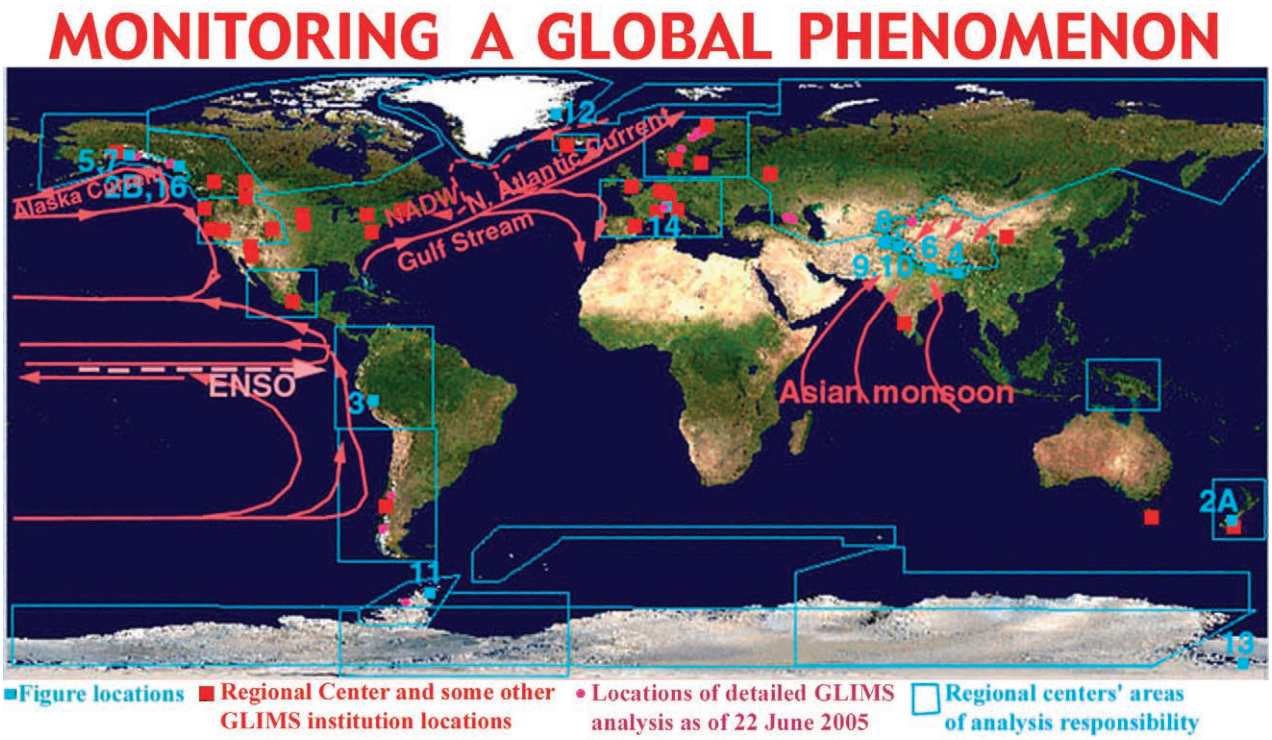
MONITORING A GLOBAL PHENOMENON
Alaska Coast
NADW
N. Atlantic Current
Gulf Stream
ENSO
Asian monsoon
Figure locations
Regional Center and some other GLIMS institution locations
Locations of detailed GLIMS analysis as of 22 June 2005
Regional centers' areas of analysis responsibility

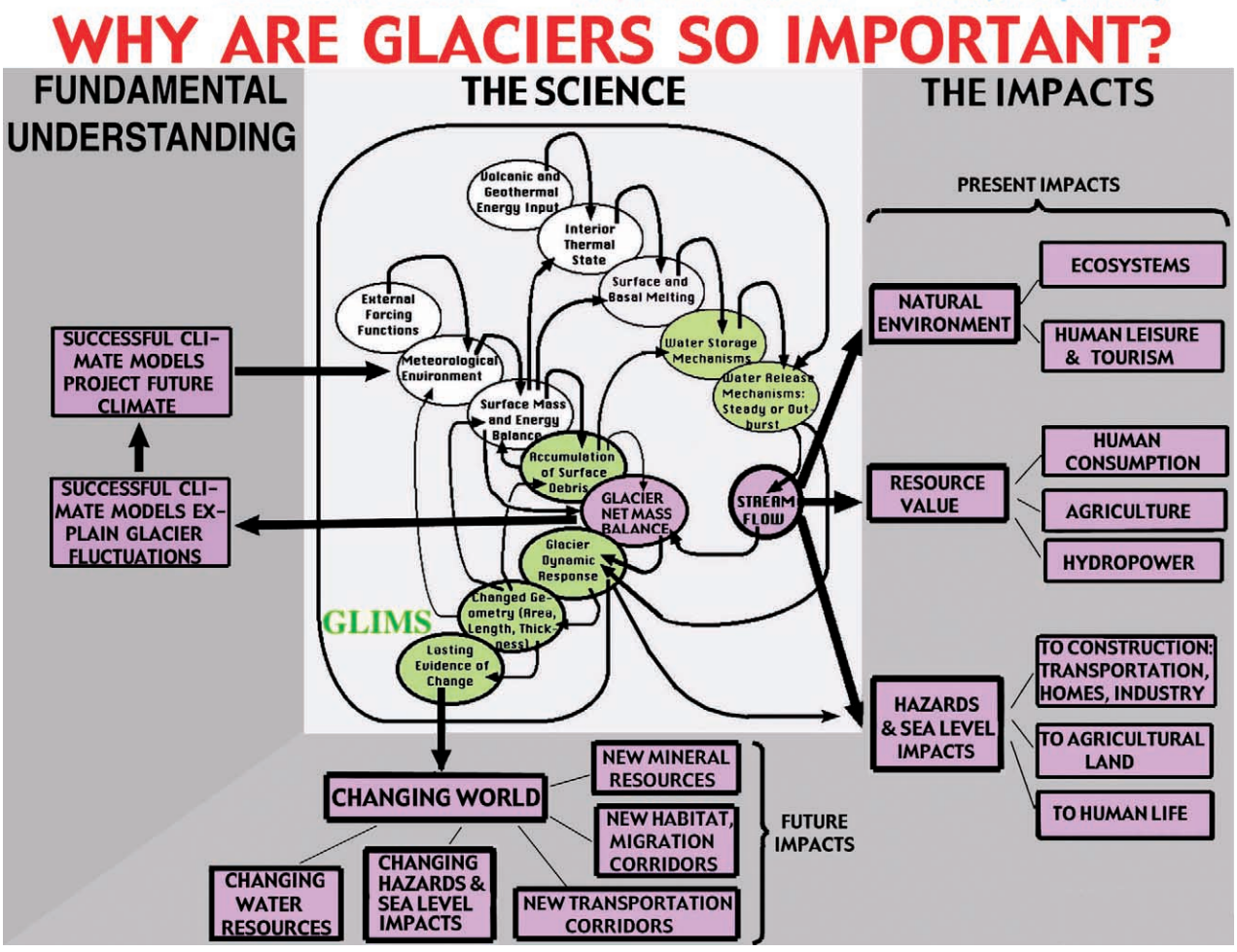
WHY ARE GLACIERS SO IMPORTANT?
FUNDAMENTAL UNDERSTANDING
THE SCIENCE
THE IMPACTS
SUCCESSFUL CLIMATE MODELS PROJECT FUTURE CLIMATE
SUCCESSFUL CLIMATE MODELS EXPLAIN GLACIER FLUCTUATIONS
Volcanic and Geothermal Energy Input
Interior Thermal State
Surface and Basal Melting
External Forcing Functions
Meteorological Environment
Water Storage Mechanisms
Water Release Mechanisms: Steady or Outburst
Surface Mass and Energy Balance
Accumulation of Surface Debris
GLACIER NET MASS BALANCE
STREAM FLOW
Glacier Dynamic Response
Changed Geometry (Area, Length, Thickness)
Lasting Evidence of Change
GLIMS
PRESENT IMPACTS
NATURAL ENVIRONMENT
ECOSYSTEMS
HUMAN LEISURE & TOURISM
RESOURCE VALUE
HUMAN CONSUMPTION
AGRICULTURE
HYDROPOWER
HAZARDS & SEA LEVEL IMPACTS
TO CONSTRUCTION: TRANSPORTATION, HOMES, INDUSTRY
TO AGRICULTURAL LAND
TO HUMAN LIFE
CHANGING WORLD
NEW MINERAL RESOURCES
NEW HABITAT, MIGRATION CORRIDORS
NEW TRANSPORTATION CORRIDORS
CHANGING HAZARDS & SEA LEVEL IMPACTS
CHANGING WATER RESOURCES
FUTURE IMPACTS

Field investigations of glaciers provide the most detailed, uncompromised, and reliable information on glacier mass balance. Only a few dozen glaciers around the world—and mainly small, simple glaciers not fully representing the world's land ice—are being assessed for mass balance, at differing levels of completeness. Because glaciers are numerous (10^5: Meier & Bahr, 1996), widespread, and mostly remote, remote sensing is needed to acquire comprehensive, uniform, and frequent global observations of glacier variations. Field-based and satellite-based glacier monitoring results so far lack the comprehensiveness needed to assess sensitivity to regional and local differences in glacier response functions. The observations must now be expanded using remote sensing (Paul & Kääb, in press; Rau et al., in press). Mass balance is difficult, sometimes impossible, to obtain by remote sensing, but surface observations by these methods can yield powerful measurements of glacier state and dynamics.

Some recent remote-sensing methods include satellite radar interferometry and radar speckle tracking of flow (Reeh et al., 2003; Rignot et al., 2004); passive microwave measurements of temperature and melt zones (Abdalati & Steffen, 2001); active microwave mapping of glacier facies, including melt zones; and airborne and satellite laser altimetry and satellite radar measurement of glacier and ice-sheet surface topographic profiles (Krabill et al., 2004; Spikes et al., 2003). Remote sensing and field studies validate the theoretical concept of size-dependent time scales of glacier responses to climate change (Baisheng et al., 2003; Huybrechts, 2002; Jóhannesson, 1985; Pelto & Hedlund, 2001). These methods also highlight anomalous fast responses of some large glaciers, ice caps, and ice sheets due to meltwater dynamics, ice-shelf unpinning and breakup, and other instabilities (Abdalati & Steffen, 2001; Abdalati et al., 2001; Bamber & Rignot, 2002; Bindschadler et al., 2003; De Angelis & Skvarca, 2003; Joughin et al., 2002, 2004; Krabill et al., 2004; Oppenheimer, 1998; Rignot et al., 2004; Rott et al., 2002; Scambos et al., 2004, 2000).

Satellite multispectral visible/near-infrared (VIS/NIR) imaging, such as by ASTER, ETM+ (Enhanced Thematic Mapper Plus), and SPOT (Satellite Probatoire d'Observation de la Terre), is needed for systematic large-scale measurements of glacier and ice sheet state and dynamics (e.g., Ferrigno et al., 1996, 1997; Frezzotti et al., 1998; Williams & Ferrigno, 2002). These measurements must be considered in the context of very rapid changes or oscillations of some glaciers (e.g., tidewater and surging glaciers) that may occur on a time scale shorter than the ASTER repeat imaging interval. Older Landsat, declassified images (Bindschadler & Vornberger, 1998), airphotos, and maps extend knowledge of glacier changes across most of the last century.

ASTER data are commonly used in conjunction with other types of remote sensing data. ASTER has unique attributes and handicaps compared to other remote sensing systems. ASTER has a stereo, same-orbit imaging capability that other systems lack. ASTER stereo-derived topography lacks sufficient vertical resolution to be useful in ASTER-to-ASTER glacier surface topography change assessment, except in extraordinary circumstances; but it is useful for comparison with reliable topographic map data where the baseline extends over several decades and to assess rapid thinning during glacier surges. ASTER topographic mapping lacks the large layover of synthetic aperture radar, but of course it cannot see through clouds; and ASTER has a higher lateral spatial resolution but lower vertical resolution compared to laser methods. ASTER stereo DEMs (digital elevation models) are being used to generate stable image orthorectifications and to map glacier lake, glacier terminus, and snowline elevations. ASTER's 90-m five-band thermal imaging is unparalleled, but has just begun to be exploited for glaciological studies. Six short-wave infrared bands (30-m resolution) are well placed spectrally to be used with three visible/near-infrared bands (15-m resolution) for ice and water detection. Other systems duplicate or exceed some of ASTER's specifications, but none duplicate the whole package for glaciological investigations.

The delineation of debris-covered glaciers is a bottleneck for rapid, automated assessment of glaciers from satellite data in some mountain areas, such as in parts of Alaska and the Himalaya. Traditional statistical multispectral classification algorithms are of limited value in these areas. For example, multispectral data analysis is challenged to discern dirty, shadowed ice from extremely turbid water or debris-covered glacier ice vs. ice-free moraines. Such glaciers can be mapped manually, although the combination of multispectral classifications with DEM derivatives and neighbourhood analysis has revealed promising avenues for semi-automated mapping (Paul et al., 2004, and references therein).

To assist the international community effort to document glacier changes, GLIMS was organized. It now involves more than 92 researchers and 62 institutions in 25 countries (some key institutions are located in Fig. 1A). The project is developed from the World Glacier Monitoring Service's World Glacier Inventory (Haeberli et al., 1998) and the USGS series *Satellite Image Atlas of the Glaciers of the World* (e.g., Williams & Ferrigno, 2002; Williams et al., in press). Here a subset of the consortium provides an update and supplement to previous reports on selected aspects of GLIMS (Bishop et al., 2004; Kääb et al., 2003a,b; Kieffer et al., 2000; Raup et al., 2000; http://www.glims.org). Technical details of our methodologies and algorithms will be presented in a separate paper (B. Raup et. al, manuscript submitted to Computers and Geoscience); more comprehensive science results will be presented in stages subsequently.

Concerns for users of the GLIMS glacier database are (1) performance comparisons for analysis using various imaging systems and other data sources (Hall et al., 2003) and (2) inter-laboratory comparisons of data quality and uniformity

using the same data sources. Standardization of analysis results is achieved partly by the common use of ASTER and similar multispectral data, and partly by the structure of the database. The database includes a set of parameters based on and expanded from those adopted by the World Glacier Monitoring Service (Haeberli et al., 1998). Testing is underway to assess systematic and individual/inter-laboratory errors in geolocation determinations, interpretation errors and differences, and errors caused by algorithmic differences and deficiencies (results to be presented elsewhere). Adherence to standards and some degree of uniformity of analysis method will be necessary before a comprehensive global assessment of GLIMS data can be presented.

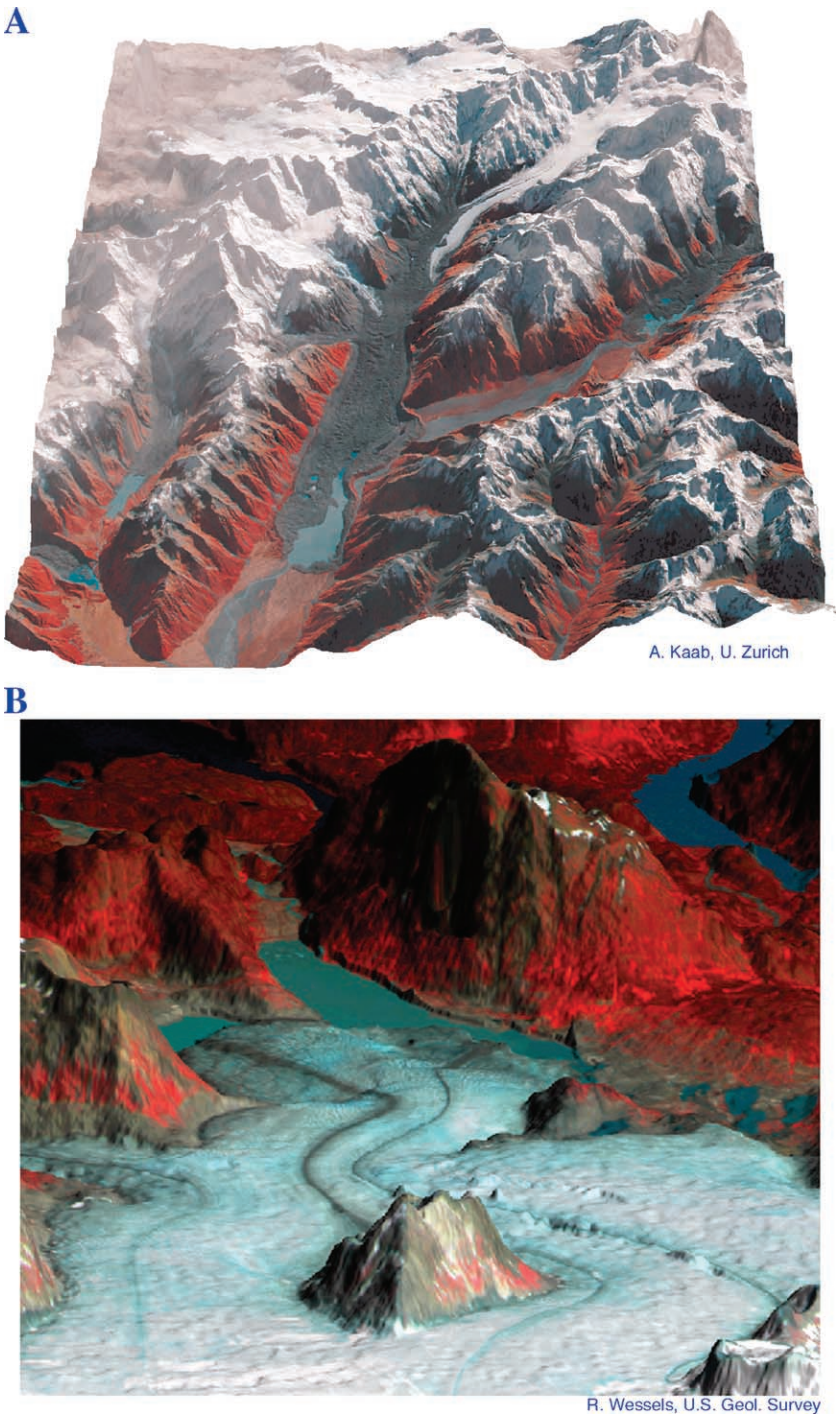

Fig. 2. Examples of ASTER RGB false-color composites draped over ASTER DTMs. (A) Tasman Glacier, New Zealand. The scene covers approximately 25 × 25 km and the view is looking northward. (B) Llewellyn Glacier, British Columbia. Scale is ~13 km across the middle of the image and 25 km from bottom (foreground) to top (background).

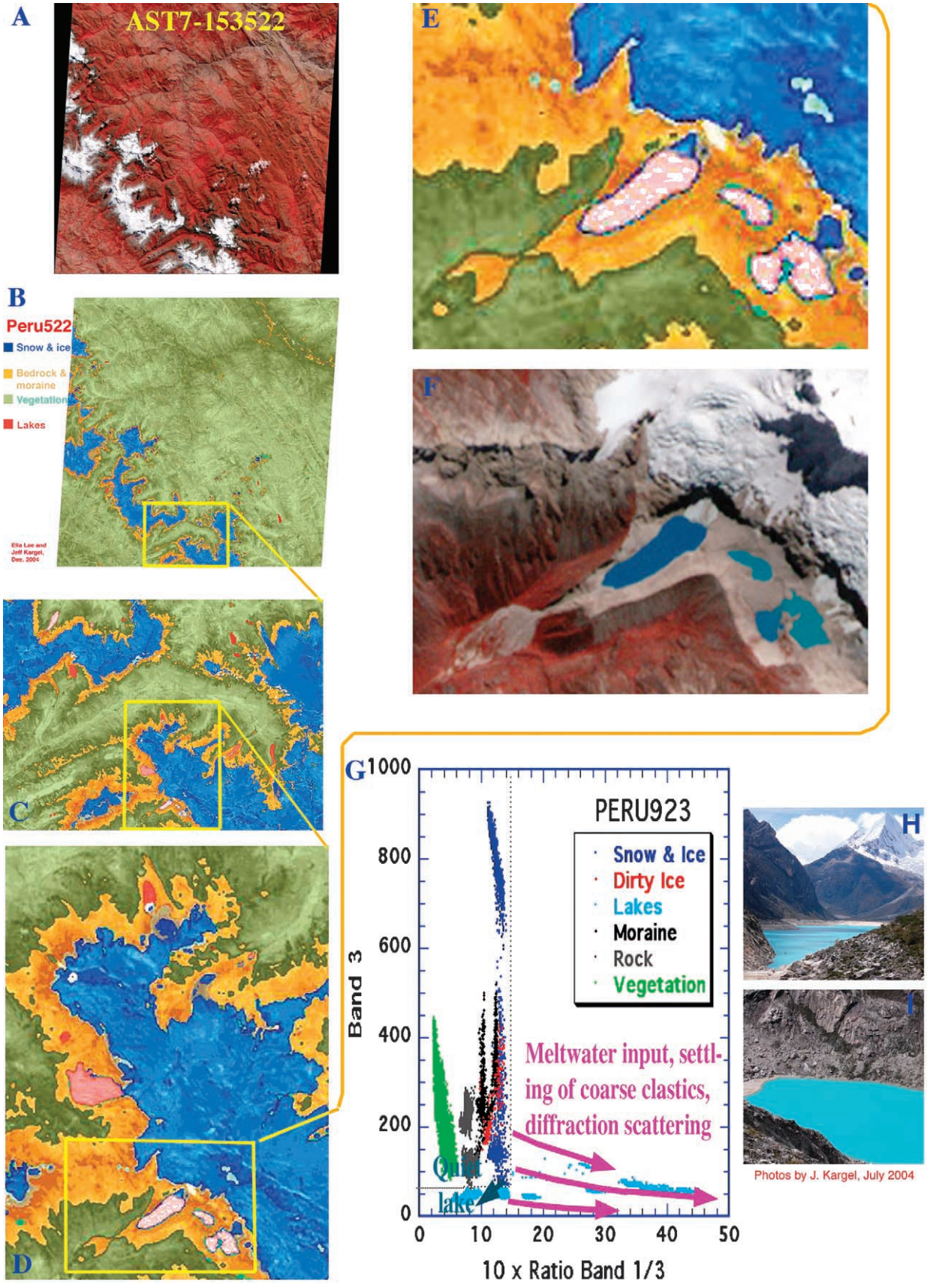
A
AST7-153522
B
Peru522
Snow & ice
Bedrock & moraine
Vegetation
Lakes
Ella Lee and Jeff Kargel, Dec. 2004
C
D
E
F
G
PERU923
Snow & Ice
Dirty Ice
Lakes
Moraine
Rock
Vegetation
Band 3
1000
800
600
400
200
0
0
10
20
30
40
50
10 x Ratio Band 1/3
Meltwater input, settling of coarse clastics, diffraction scattering
Quiet lake
H
I
Photos by J. Kargel, July 2004

2. GLIMS technology development summary

2.1. Terrain classification

DEMs are useful for visualization of glacier data and ASTER imagery (Fig. 2) and are needed for atmospheric corrections of satellite imagery (Bishop et al., 2004), geometric orthorectification of satellite images (Kääb, 2002, 2005; Kääb et al., in press), derivations of 3-D glacier parameters (Kääb et al., 2002; Paul et al., 2003, 2002), multidimensional classification of debris covered ice (Paul et al., 2004), and other geomorphometric tasks (Bishop et al., 2004). Accurate orthorectification of satellite data is mandatory in order to allow the combination of multi-year satellite data sets and to enable fusion with DEM data and other georeferenced data sets. Under favorable circumstances, stereo satellite images can be used to measure vertical thickness changes in glaciers, and multi-temporal satellite imagery can be used to make estimations of glacier mass balance (Berthier et al., 2003, 2004). More commonly, the topographic (vertical) resolution limit of satellite stereo-derived DEMs (digital elevation models) reduces the value of these topographic data sets for glacier change analysis. ASTER imagery is more useful for measurements of changed length, area, and surface facies.

This may be difficult to achieve in parts of the world with poor topographic maps. Partly relieving this deficiency, DEM data are available for free from the SRTM mission (Rabus et al., 2003), and the stereo capability of ASTER also allows DEM creation (Kääb et al., 2003a).

Ideally, mutispectral classification of material units is done on imagery that has had raw radiance values corrected to yield albedos or reflectances, with effects of shadows, adjacent terrain, and atmospheric air mass removed. This has been done on a test basis at the University of Nebraska at Omaha, but more often these corrections have not been made before multispectral classification is done. A deficiency of artifact- and hole-free DEMs remains a serious problem and challenge.

In Fig. 3, an example from Peru's Cordillera Blanca, terrain classes are mapped using a simple algorithm based on supervised cluster assessment of ASTER band 1/band 3 ratios and band 3 radiance. Many details of the classified output in Fig. 3, which might be overlooked as noise or artifacts, were field-validated as small melt ponds and ice cliffs of calving debris-covered glaciers. Fig. 3 also highlights a long-recognized limitation of multispectral terrain classification. The actual glacier boundaries are not well mapped where they are heavily debris covered, especially where debris-covered ice abuts talus slopes or old moraines. However, some discrimination is possible because supraglacial debris tends to be less weathered and less vegetated than other types of surficial debris and exposed bedrock.

The delineation of debris-covered glaciers and rock glaciers in many high-relief alpine environments is a bottleneck for their rapid, automated assessment from satellite data (Bishop et al., 1995; Paul et al., 2004; Wessels et al., 2002). In parts of Alaska, the Andes, and the Himalaya, traditional statistical multispectral classification algorithms are of limited value because of inherent difficulties in using pure multispectral data to separate, for example, dirty, shadowed ice from extremely turbid water, or to separate debris-covered glacier ice from ice-free moraines. Natural variations in illumination and surface conditions in alpine regions may introduce further errors in classified output. Additional information provided by DEMs (Bishop et al., 2001), neighbourhood analysis (Paul et al., 2004) and thermal radiation (Taschner & Ranzi, 2002) sometimes enables mapping of debris-covered glaciers. Sophisticated approaches to information generation, data fusion, and classification, including neural net-based techniques, have been successfully applied by GLIMS to handle some of these difficult problems (Bishop et al., 1999, 2004; Kääb et al., 2002; Paul et al., 2004).

2.2. Glacier surface velocity mapping

The surface velocity field is a key glacier dynamic quantity mappable with multitemporal orthorectified ASTER, Landsat ETM+ and older Landsat TM and MSS data, and SPOT imagery using different correlation techniques (e.g., Fig. 4 and Dowdeswell & Benham, 2003; Kääb, 2002, 2005, in press; Lucchitta & Ferguson, 1986; Raup et al., 2001; Scambos et al., 1992; Skvarca et al., 2003).

2.3. Use of historic map data with ASTER and other satellite data

Historic map data can be coregistered to a single classified glacier image to obtain change information over decadal periods. Recent maps can fill gaps in satellite coverage, and older maps can extend coverage to the pre-satellite era. This is a critical activity of the glaciological community, e.g., quantitative comparisons, with error assessments, of historic map data with satellite imagery

Fig. 3. ASTER scene acquired over Cordillera Blanca, Peru, highlights some mapping capabilities using a simple classifier ("B3R13") based on ASTER band 1/ASTER band 3 ratios and ASTER band 3 radiances. (A) RGB band 3-2-1 false-color composite of a radiance-calibrated image used for the analysis. (B) Classified image output. (C, D, and E) Enlarged sections of the classified image. Each material unit is mapped with various hues of a different color. For instance, lakes are mapped in reddish hues: pink, salmon, and red; the lighter pink tones portray brighter band 1 radiance (light pastel blue or turquoise colors to the human eye); darker reds portray low radiance values and are clear, dark lakes to the human eye. Even shadowed areas—whether rock or snow or ice—appear to be well classified. (F) RGB composite showing details corresponding to the classified output in E. (G) The same parametric thresholds and classifier functions did well in separating material classes of another test scene over a nearby part of the Cordillera Blanca. (H and I) Two typical pastel-turquoise glacier lakes in Cordillera Blanca.

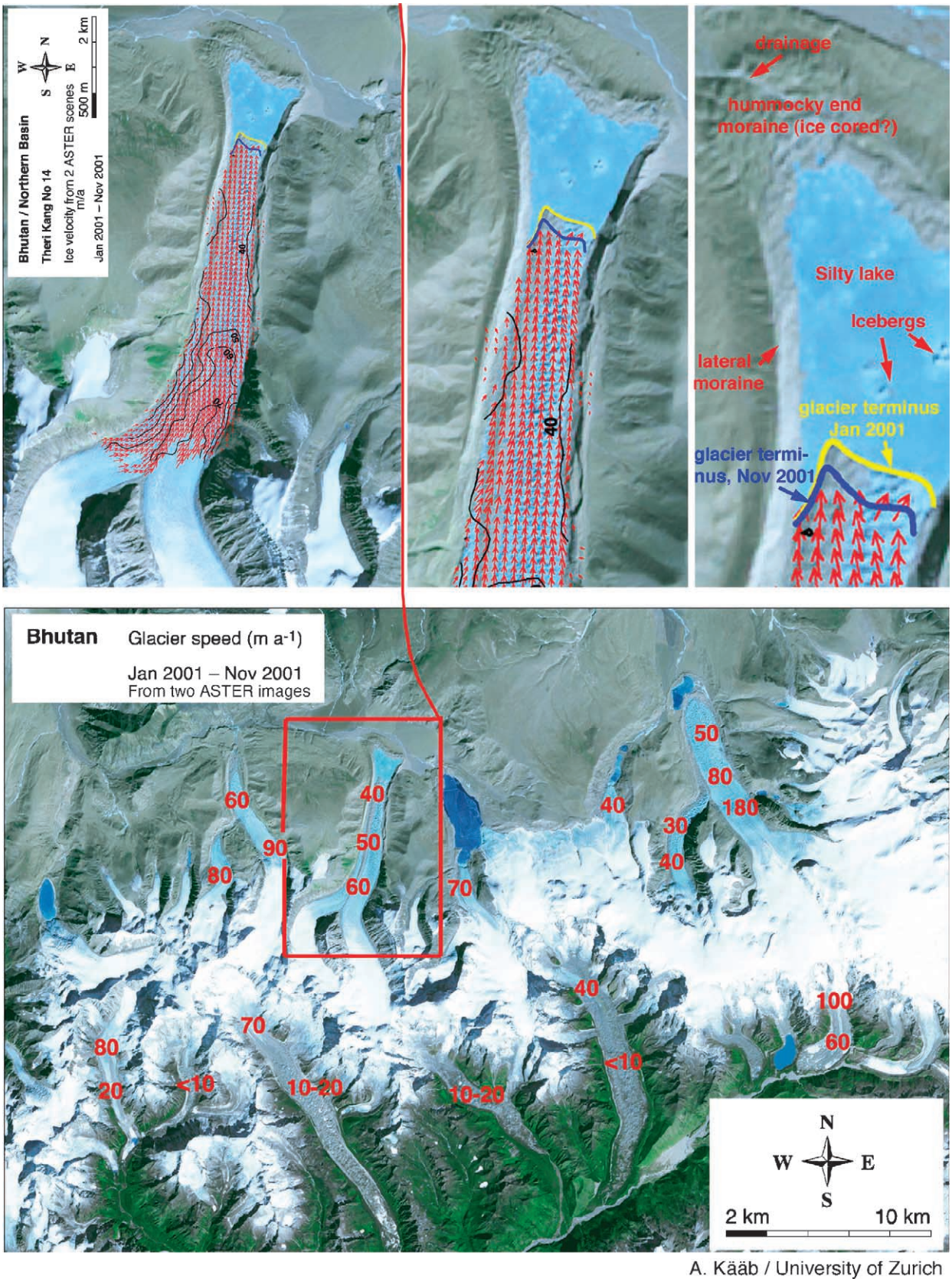

Fig. 4. Surface displacement vector fields determined by feature tracking in two ASTER scenes acquired 10 months apart in 2001 over the eastern Himalaya, Bhutan. Red numbers in lower panel are representative velocities, m/year.

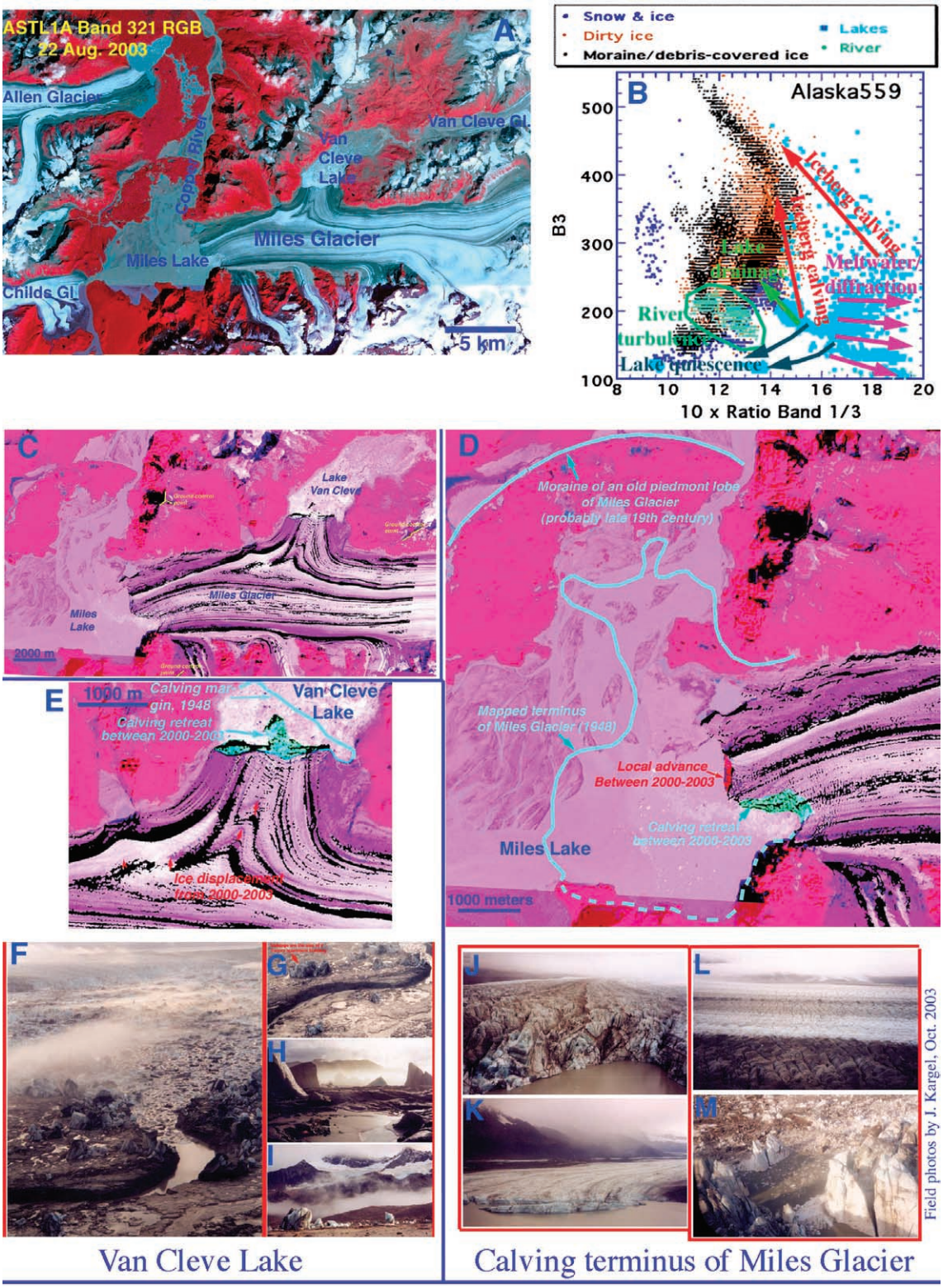

Fig. 5. (A) ASTER band 3-2-1 RGB false-color composite showing the glaciers of the Copper River region, Chugach Range, Alaska, Aug. 22, 2003. (B) Scatterplot shows material classes based on supervised classification. Classification output involves overlapping fields and highlights some limitations of multispectral data for terrain classification. (D, E): Rubber-sheeted USGS topographic series map data (data inputs from 1948) registered to a 2000 Landsat 7 ETM+ scene and a 2003 ASTER image reveals changes across 55 years. (F–I) Van Cleve Lake in October 2003; Miles Glacier in background of (F). (J–M) Calving terminus of Miles Glacier in Miles lake (a widening of the Copper River).

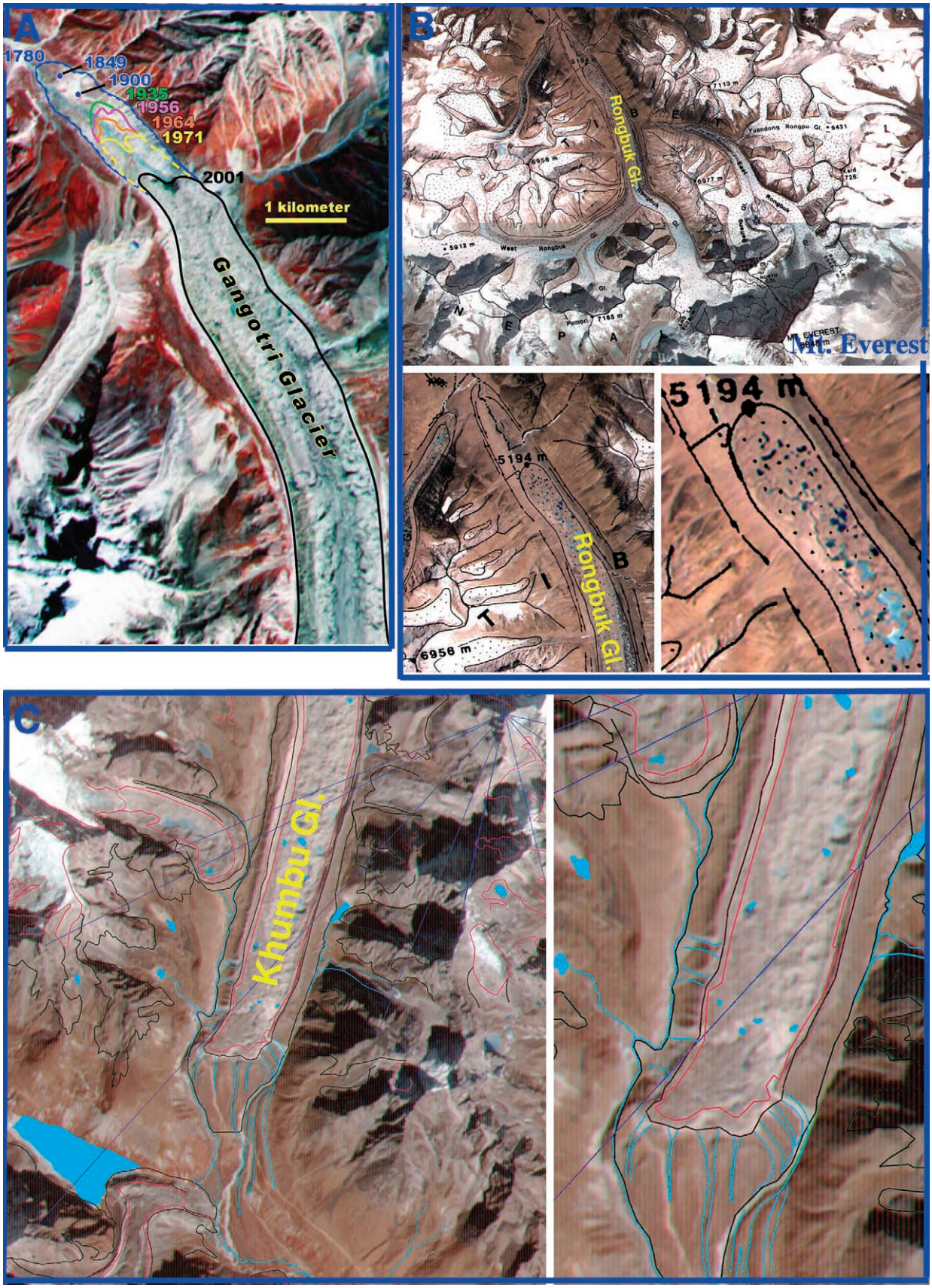
A
1780
1849
1900
1935
1956
1964
1971
2001
1 kilometer
Gangotri Glacier
B
Rongbuk Gl.
Mt. Everest
5194 m
6958 m
C
Khumbu Gl.

(e.g., Hall et al., 2003). Use of paper map data presents unique challenges, and commonly requires "rubber sheeting" in the best circumstances, and is useless for quantitative work in the worst cases. Product reliability sometimes can be gauged by the registratability of immobile tie points. Some map data are geodetically fairly accurate, but glaciers can be misinterpreted or confused with snow fields, sea ice, etc. Fig. 5 is a simple example of glacier change assessment of the Miles Glacier (Alaska) made on the basis of 1948 map data with an ETM+ image from 2000 and an ASTER image from 2003. Further examples are shown for Himalayan glaciers in Fig. 6.

2.4. Use of thermal mapping to aid glacier lake interpretation

Thermal imaging of glaciers is useful to identify glacier facies (Taschner & Ranzi, 2002). Thermal methods of material discrimination may involve (1) thermal inertia measurements if looks at multiple times of day can be provided (generally not by ASTER), (2) differential heating at a single time in one morning look (possible with ASTER), and (3) observation of the thermal buffering by the enthalpy of melting of H_2O. Fig. 7 shows iceberg-cluttered lakes at the termini of Alaskan glaciers; those icy lakes stand out in contrast to the warmer land and debris-covered parts of glaciers, because these lakes have temperatures close to freezing. Relative to the ice point, some lakes have a 1–2 K positive anomaly, which is slightly greater than typical TIR calibration errors of order 0.8 K. Other lakes near the stagnant terminus of the debris-covered Martin River Glacier are variously cold and warm (Fig. 7), indicating variations in the degree of thermal interaction between ice and water.

2.5. GLIMSView

GLIMSView is an open-source, cross-platform application intended to aid and standardize the process of glacier digitization for the GLIMS project and packaging that information for transfer to the National Snow and Ice Data Center for ingestion into the GLIMS Glacier Database. It allows users to view various types of satellite imagery, digitize glacier outlines and other material units within the images, attach GLIMS specific attributes to segments of these outlines, and save the outlines to ESRI shapefiles for ingestion into the GLIMS Glacier Database. GLIMSView continues to undergo development. It is free and available at http://www.glims.org/glimsview/.

2.6. GLIMS glacier database

The GLIMS database (Raup et al., 2001) represents time-varying geospatial information about a set of objects, which in some cases have tree-like interrelationships. The GLIMS glacier database has been designed to follow directly from the World Glacier Monitoring Service and World Glacier Inventory (Haeberli et al., 1998). The analyses producing this new information are performed using a variety of input sources (satellite imagery, airphotos, and maps) and methods, including automatic algorithms and manual interpretation. A standardization protocol is being developed and implemented in GLIMSView, but some manual editing and human choice of automatic processing tools—hence, subjective interpretation—remains in the resulting data. This information comes from many researchers from around the world. A wealth of metadata about the analyses and the analyst must be accommodated. The results of glacier analysis at the Regional Centers are sent to the National Snow and Ice Data Center in Boulder, Colorado, USA, which designed and maintains the database.

NSIDC has implemented the GLIMS Glacier Database using the Open Source tools including PostgreSQL, PostGIS, and MapServer. The interface to the database provides various types of search capability, and also functions as an Open Geospatial Consortium (OGC)-compliant Web Map Service (WMS) and Web Feature Service (WFS), serving map layers to other Web map servers.

3. Science applications

3.1. Glacier change in Afghanistan and Pakistan

Snow and ice in large parts of Afghanistan and Pakistan are the main source of irrigation waters. Ever since the Indus Valley civilization glaciers have been key in the region's human story (Hewitt, 1961). Remote-sensing assessment of the region's cryosphere can contribute to enhancement of regional security and well being through improved knowledge of present and future melt-water resources. The region's alpine glaciers are diverse in type, dynamics, size, and debris cover. These attributes and strong regional variations in topography and monsoonal influences affect glacier state and sensitivity to climate change.

Satellite-based assessments using Landsat Multispectral scanner data, coupled with topographic maps made from aerial photographs and field campaigns, represent baseline information on Afghanistan's glaciers 30–40 years ago. The

Fig. 6. Rubber sheeted glacier terminus lines overlain on ASTER images of debris-covered glaciers in the central Himalaya. (A) Map data registered to an ASTER image of Gangotri Glacier, India, shows long-term recession. (B) Changes in Rongbuk Glacier, Tibet, just northwest of Everest, between 1986 map (from Burbank et al., 1996) and 2001 ASTER. (C) Changes in Khumbu Glacier, Nepal, just southwest of Everest, between 1958 map data and 2001 ASTER; map lines are rendered from slope-related shadings in the 1958 map data. The termini of Rongbuk and Khumbu Glaciers have been stably positioned against end moraines; field observations show the glaciers to be downwasting and losing mass. Rongbuk Glacier exhibits numerous supraglacial lakes (not to be confused with the black stipples on the Rongbuk from the original map).

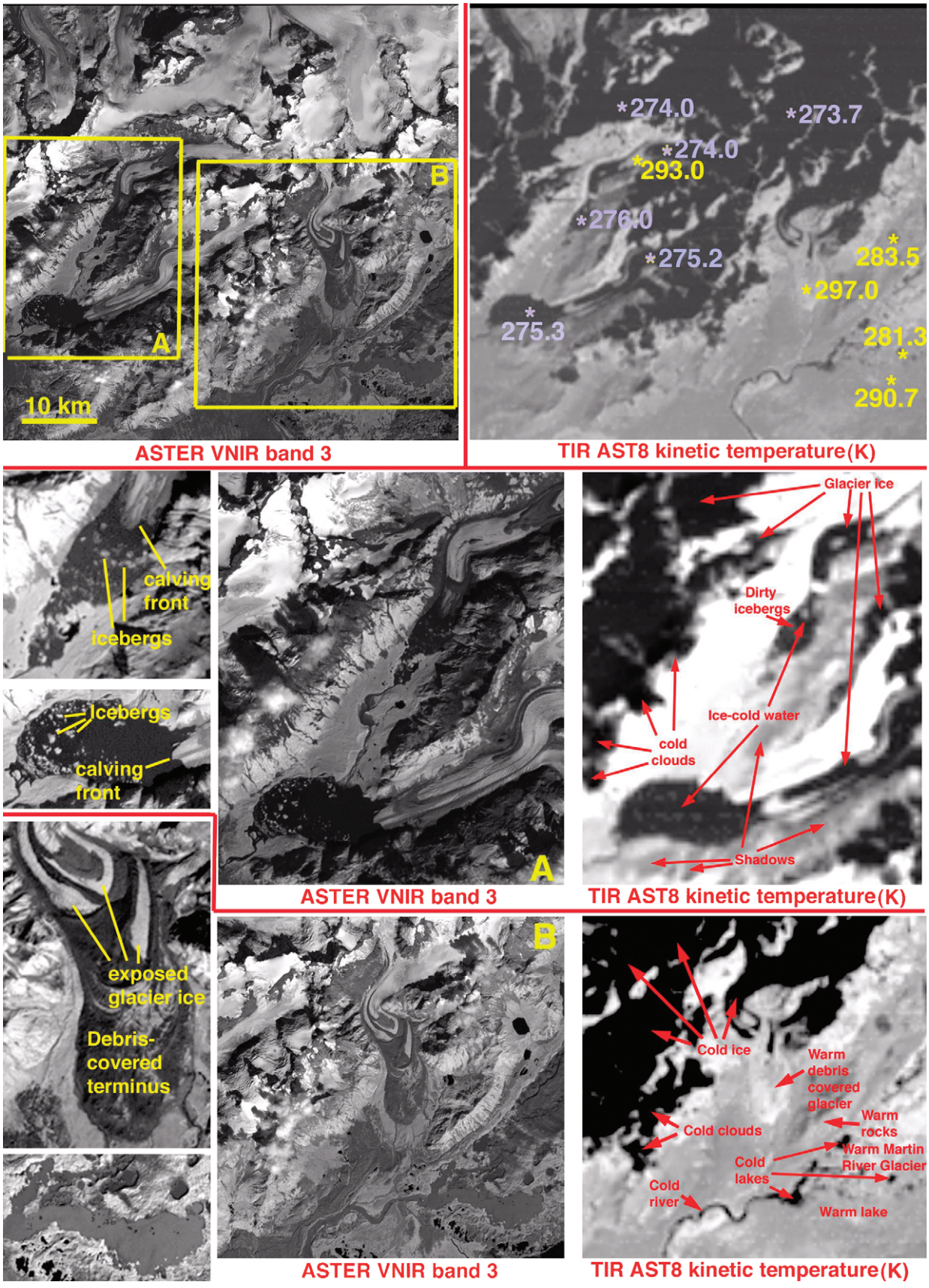

Fig. 7. Comparison of ASTER VNIR and temperature images of glaciers east of the Copper River, Chugach Range (Alaska). Spot measurements show kinetic temperature in K.

baseline has been updated with ASTER and other imagery (Shroder & Bishop, in press-a,b). Additional field investigations and remote sensing and GIS studies allow preliminary assessment of glacier fluctuations in northern Pakistan (Shroder & Bishop, in press-a,b).

The glaciers of Afghanistan were mapped as a part of country-wide topographic mapping by the USA and USSR (Shroder, 1983). Additional information and assessments came through expeditions, the Atlas of Afghanistan Project (Shroder, 1975), the UN-sponsored World Glacier Inventory, and the USGS-sponsored *Satellite Image Atlas of the Glaciers of the World* (Shroder & Bishop, in press-a,b). The total glacierized area of the Hindu Kush of Afghanistan and western Pakistan was estimated at ~6200 km^2 (Horvath, 1975). Over 3000 small glaciers were inventoried in Afghanistan. Most existed below the climatic snowline and survived in strongly shadowed areas, places receiving windblow and snow avalanches, or where protected beneath thick debris cover. Most glaciers of Afghanistan occur on north-facing slopes; in the northeastern part of the country they occur with the highest peaks, greatest monsoon precipitation, and most extensive cloudiness associated with the Intertropical Convergence Zone (ITCZ).

Despite the general metastability of most of Afghanistan's small glaciers and the severity of recent regional climate change including drought, glacier changes have been minor compared to changes occurring elsewhere in the world; but there have been changes (examples below). A small number of Afghanistan's glaciers have disappeared entirely in recent decades; others have downwasted, retreated, and divided into multiple daughters so that the overall total number of ice masses may not have changed much.

About 18 small (<~0.5 km^2) glaciers occurred in the Koh-i-Baba range of central Afghanistan about half a century ago (Shroder & Giardino, 1978). The lowest elevations of exposed glacial ice were ~4075–4657 m (average ~4365 m). Foladi Glacier (Fig. 8) in 1978 had a 20–25% reduction of surface area of exposed ice since the 1959 aerial photographs. Mean annual snowfall in that period was ~600 mm and the climatic snowline was ~5100 m. Stereo ASTER imagery in 2003 shows the glacier to be further downwasted and now deeply incised behind its recessional moraine; however, the terminus and marginal positions of glaciers in this region have not changed much (Fig. 8).

Near Mir Samir Peak (5809 m, north-central Hindu Kush), East and West Glaciers were assessed by the British in 1965 (Gilbert et al., 1969), who studied snow accumulation, ablation, melt-water discharges, lichenometry, and heat balance. They also made planimetric maps that now enable comparison with ASTER imagery. East Glacier then measured ~1 km^2 and West Glacier ~0.5 km^2; in 2003 both glaciers had retreated significantly and formed new lakes inside their end moraines. A small glacier adjacent to the northwest side of West Glacier was topographically mapped from air photos in 1959, was only a small patch in 1965, and is now entirely melted away.

The Keshnikhan Glacier in the Wakhan Corridor in northeast Afghanistan was mapped in 1970 (Braslau & Bussom, 1978). It is ~15 km^2, 4 km long, and steep, with a continuous belt of morainal debris from 2600 m elevation near the Ab-i-Panj river valley, to the ice front almost 2000 m higher. Braslau and Bussom (1978), and Shroder (1978) considered the glacier to be receding. Further changes are minimal up to the present, according to ASTER image analysis.

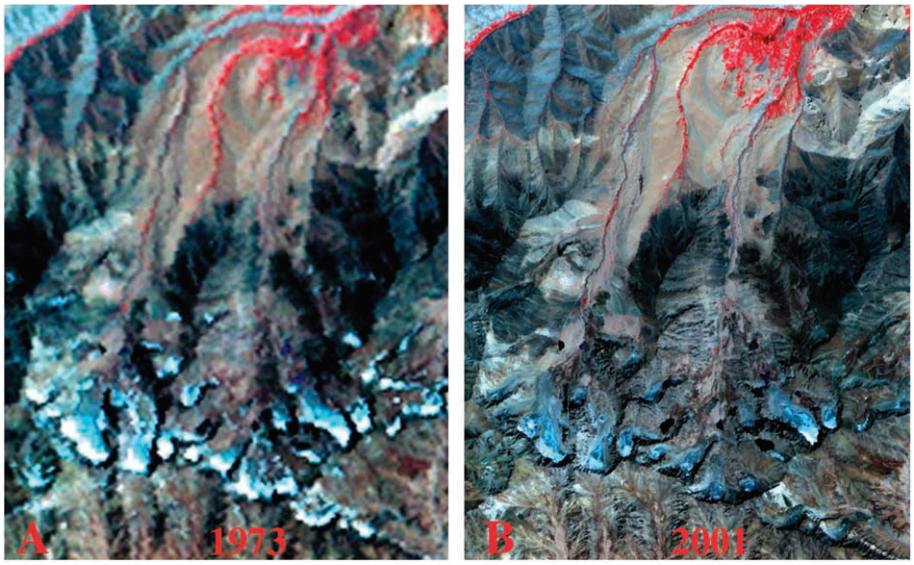

Fig. 8. (A) MSS image (80 m resolution) of Foladi Glacier (Afghanistan) in 1973. (B) ASTER image of Foladi Glacier in 2001. Even with the large difference in spatial resolution, it can be seen that there is less ice in the later image, although the difference is less than found among many other glaciers of this size elsewhere in the world.

Despite annual precipitation < 100 mm year^{-1} (Lalande et al., 1974) the predominant high altitude (5000–>6000 m) in the Wakhan Pamir has allowed some of Afghanistan's largest glaciers to develop, including the Northern and Southern Issak and Zemestan glaciers, which were mapped in 1975 (de Grancy & Kostka, 1978). Transient snowlines in August 1975 averaged ~5100 m. No significant changes have been noted in ASTER imagery compared the 1975 data.

In Pakistan, baseline information from expeditions and remote-sensing studies provide a preliminary assessment of individual glaciers (e.g., Bishop et al., 1995, 1999, 1998; Miller, 1984; Searle, 1991). Many glaciers have been retreating (readily seen in satellite imaging) and/or downwasting (not clearly discerned by satellite imaging, except by surface texture changes, debris cover changes, and lake formation). For example, using ASTER and field imagery we have identified a disconnection in glacier flow in the Hindu Kush between the upper and lower Tirich Mir Glaciers (Fig. 9). Landsat TM imagery in 1995 and newer ASTER imagery also indicates the development of new supraglacial lakes on the upper Tirich Mir Glacier.

A high frequency of small supraglacial lakes occurs on the Baltoro Glacier near K2 in the Karakoram Himalaya. Smaller glaciers in the Nanga Parbat Himalaya exhibit fewer supraglacial lakes, although on the south side of Nanga Parbat, some glaciers (e.g., Tap) have large lakes at their termini; others (e.g., Shagiri, Sachen) had small lakes that recently drained. The pattern at Nanga Parbat appears to be mostly downwasting of the surface rather than terminus retreat. This is also the general pattern observed among most large valley glaciers farther east in the Himalaya of Nepal and Bhutan, where large supraglacial and proglacial lakes have developed and glaciers have wasted behind high end moraines (Fig. 4). For example, comparison of map data and SPOT panchromatic and ASTER imagery reveals that the terminus position of the Raikot Glacier (north side of Nanga Parbat) has not significantly changed much in decades. Two tributary glaciers, Ganalo and the Chongra-Raikot, however, previously were connected to the Raikot Glacier, but have separated.

Fig. 10 documents the rapid advance of the Liligo Glacier tributary to the Baltoro Glacier; the advance may be related to a strong mass balance fluctuation or an extended "slow surge." Field studies by Michael Bishop and John F. Shroder, Jr. in July 2005 showed the existence and sudden drainage of a large supraglacial lake at the new, stagnating junction of these two glaciers. Analysis of ASTER multispectral scenes in other regions of the Karakoram document surges associated with the Pumarikisk Glacier tributary to the Hispar Glacier in Hunza (Searle, 1991), and the Khurdopin Glacier in the Shimshal Valley in Hunza (Shroder & Bishop, in press-a,b).

3.2. Heterogeneous glacier changes in the Antarctic Peninsula

The northern Antarctic Peninsula is dominated by an alpine glacial system consisting of an ice cap covering the central plateau region, which feeds numerous outlet glaciers draining to both sides of the peninsula. The majority of these flow into ice shelves or terminate as tidewater glaciers. In addition, isolated ice caps, mountain glaciers and ice piedmonts characterise the margins of the peninsula and the adjacent islands. In contrast to the usual slow reaction of continental ice masses, the relatively small glaciers on the Antarctic Peninsula react with short response times (time scale: years to decades) to perturbations of their accumulation and ablation processes; thus, recent climate warming is already being signaled by these glaciers' responses.

Long-term surface air temperature records revealed a significant regional temperature increase of 0.02–0.07 K year^{-1} over the last five decades for both the western and the eastern sides of the Antarctic Peninsula. In particular, the warming rates identified on the western coast of the Antarctic Peninsula are substantially greater than those found elsewhere in Antarctica. Changing precipitation regimes on the Antarctic Peninsula can be deduced through the analysis of synoptic observation records and proxies. These changes, apparent in the Antarctic Peninsula's climate system in recent years, directly result in fluctuations in the annual glacier mass and energy balance cycles. As observational evidence grows, the grounded and floating parts of the local glacial systems are found to be more spatially and temporally variable than was previously expected. Among the most spectacular of these events, the disintegration of several ice shelves has taken place over the last two decades (Rott et al., 2002;

Fig. 9. SPOT image and ground photo of Tirich Mir showing detached tributary.

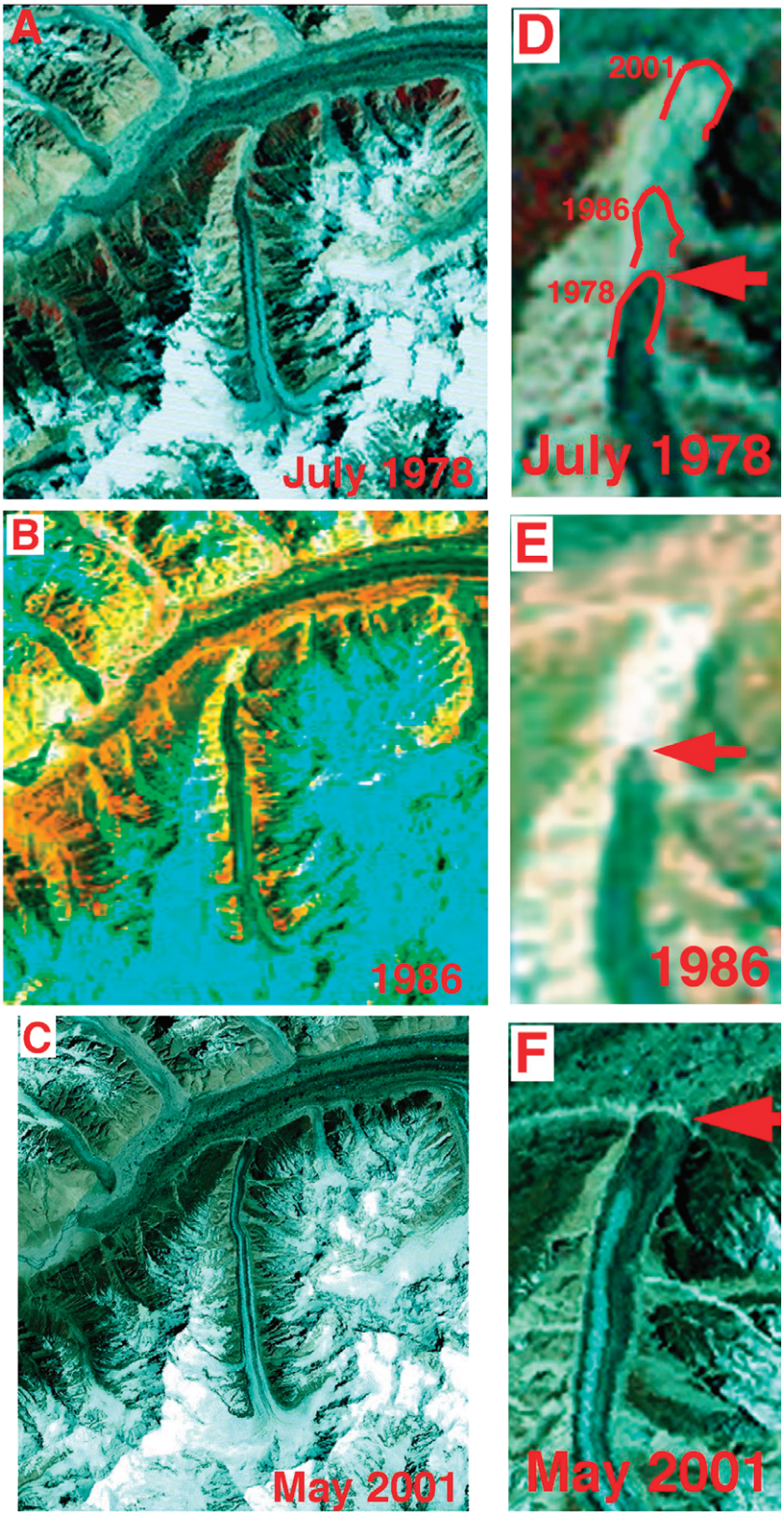

Fig. 10. Advance of Lilago Glacier. (A) Landsat MSS false-color composite of Liligo Glacier. (B) Landsat TM scene. (C) ASTER false-color composite. (D, E, and F) Closeups of the terminus region. The 2001 image shows a Type III junction, as described in Section 3.5.

Scambos et al., 2000). Furthermore, recent studies have revealed that the former tributaries have been subject to significant changes after the collapse of the ice shelf. These include recessions of the ice-fronts from the former grounding line positions, complex crevassing, thinning, flow acceleration, and higher mass fluxes (De Angelis & Skvarca, 2003; Rott et al., 2002; Scambos et al., 2004).

Analysis of high resolution ASTER data co-registered to a digital Landsat TM mosaic from the Geoscientific Information System Antarctica (GIA; Bennat et al., 1998) provides information on glacier variations between 1986 and 2002 (Rau et al., in press). In regional case studies, which cover a variety of glacial systems distributed over the northern Antarctic Peninsula, 313 glaciers were investigated. Of these, 40 (13%) had advancing glacier fronts and a total gain of 7.1 km^2, while 171 (55%) showed retreating ice fronts and a loss of 146.1 km^2. In addition, 102 (33%) were unchanged. The analysed glaciers displayed no indications of dynamic flow instabilities, and so the observed glacier variations are interpreted as the impacts of changing climate on accumulation and ablation.

Beyond the overall tendency of retreating ice fronts, spatial patterns of glacier variations are observed throughout the mid 1980s to 2001. In particular, an area of significant retreat is concentrated on the northeastern sectors of the peninsula (eastern coast of Trinity Peninsula and James Ross Island). Similarly, a predominance of glacial recession occurs along the southwestern coasts of the study area (Graham Coast, Loubet Coast and Marguerite Bay). This is contrasted with slight recessions and minor advances of glacier frontal positions that were recorded in the northwestern parts of the Antarctic Peninsula, which are exposed to the Bellingshausen Sea (western coast of Trinity Peninsula and Danco Coast). These observations from the northwest, which are presumed to be in the natural range of frontal fluctuations of tidewater glaciers, suggest relative dynamic stability of the glacial systems in this sector.

With long-term observations lacking from most parts of the Antarctic Peninsula, the high data availability on James Ross Island offers the possibility for a continuation of previous glacier monitoring activities (Fig. 11). Analysing the glacial variations on a larger perspective, a drastic acceleration of glacier recession could be determined on the island since 1988. In comparison to a retreat rate of 1.84 km^2 year^{-1} in the period of 1975 to 1988 (Skvarca et al., 1995), the annual reduction of glaciated areas doubled to 3.79 km^2 year^{-1} in the subsequent years (1988–2001). Moreover, contrary to the situation in 1988, the majority of glaciers

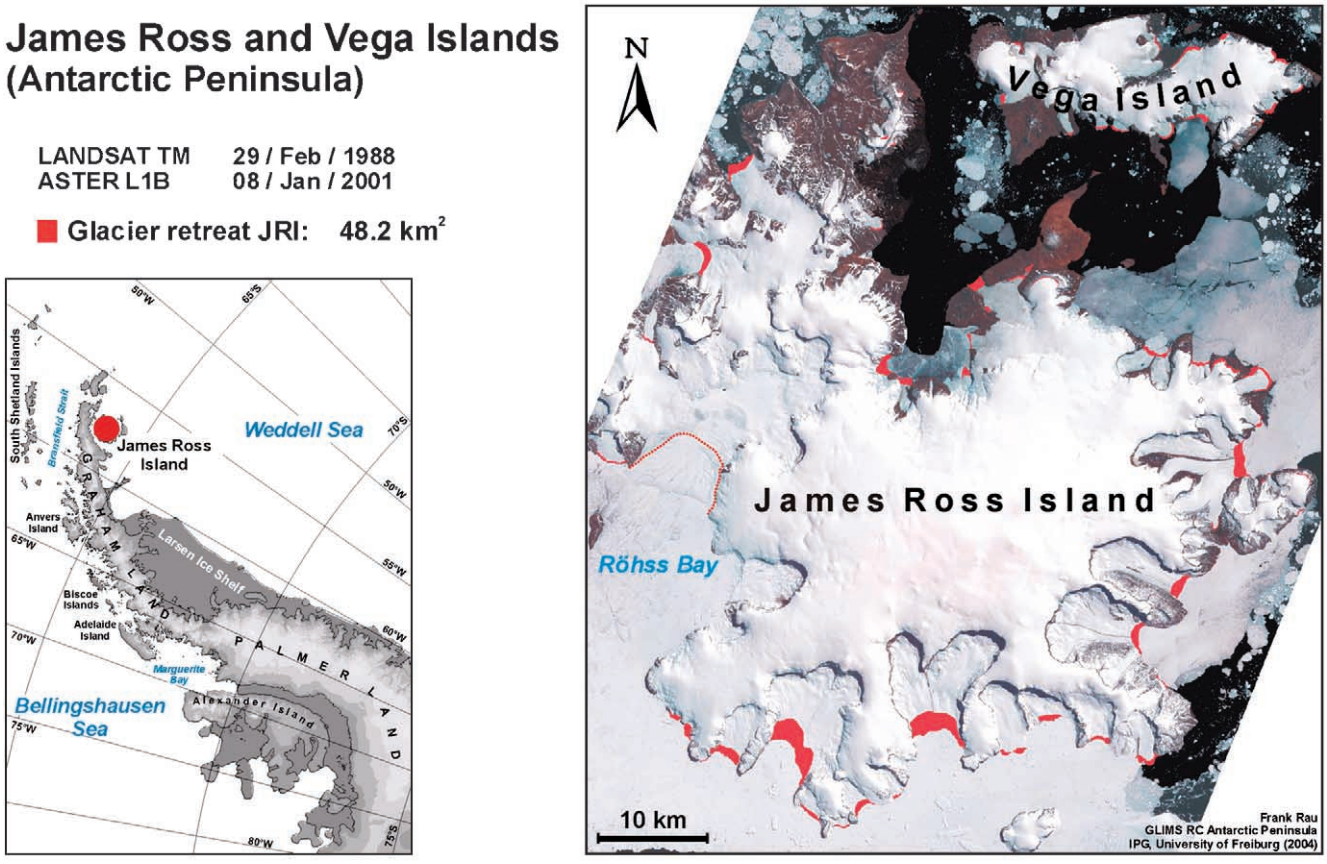

Fig. 11. Glacier retreat on James Ross and Vega Island, Antarctic Peninsula. Of 58 individual glaciers (mainly maritime) investigated during the period from 1988 to 2001 on James Ross Island, only one showed a slight advance of the glacier front; all others were subject to significant retreat, accounting for a net loss of area of 48.2 km^2. Highest retreat rates were observed on glaciers with floating ice tongues, while the 22 glaciers investigated that terminate on land lost only 2.7 km^2. ASTER image, January 8, 2001.

terminating on land in 2001 are now retreating. Over the entire period between 1975 and 2002, the glaciers on James Ross Island are found to have decreased by 78.8 km^2 corresponding to 3.9% of the previously ice-covered area.

These observations add further details regarding impacts of recent rapid climate changes—some of the most rapid rates of climate change recorded anywhere—to the Antarctic Peninsula's cryosphere. Spaceborne sensors such as ASTER and new data acquisition and distribution strategies have led to a better coverage of the polar regions with satellite data in space and time, thus providing the required tools to accomplish a functional monitoring program relevant to the field of climate change.

3.3. Polar glaciological applications of ASTER imagery

Polar remote sensing by satellite started with the Corona program of the early 1960s. High-resolution imagery to latitude ~81° North and South has been available since the 1980s from the Landsat and SPOT missions. A major milestone was the collection by Radarsat-1 in 1997 of the first continent-wide high-resolution image mosaic of Antarctica. The recent acquisition of ASTER imagery continues the collection of high-resolution visible data over the polar regions, and extends coverage to latitude ~86° North and South; another advantage afforded by ASTER is the acquisition of same-orbit along-track stereo; a third advantage is the acquisition plan, which allows for annual and more frequent imaging, a feature of the ASTER mission that has been successful mainly just for the polar ice sheets.

Ice sheet flow speeds are usually slow (10 m/year or less), except in outlet glaciers and ice streams where flow speeds can reach 500–10,000 m/year. These outlet glaciers are the dominant components of mass loss on both ice sheets, and so changes in the flow dynamics of outlet glaciers can have large mass balance implications for ice sheets. Several studies have involved the application of an automated feature-tracking routine to sequential pairs of ASTER images to derive the surface flow fields and changes in the flow fields of large polar outlet glaciers. The technique is a modification of the cross-correlation algorithm developed by Scambos et al. (1992) for low-slope ice streams in West Antarctica. In contrast to ice streams, outlet glaciers flow through rugged mountain terrain and have relatively steep surface slopes. These characteristics necessitate image ortho-rectification, which is accomplished by constructing a relative DEM using the stereo bands 3N and 3B of the ASTER sensor. The cross-correlation technique involves matching brightness features (crevasses) from one image to the next, so both images must have similar illumination. This is not always the case for ASTER imagery because of the sensor system's capability for off-nadir scene acquisition (up to 8.58° off nadir). Experiments conducted over regions of rugged relief, such as the Transantarctic Mountains, indicate that pointing angles of sequential images should be within 3° (Stearns & Hamilton, in press) to maintain common illumination necessary for the successful application of the cross-correlation algorithm.

Two examples of the application of this technique using ASTER imagery are presented for Greenland and Antarctica. Sequential ASTER images from the summers of 2001 and 2002 were used to map the surface flow field of Daugaard Jensen Gletscher, one of the largest outlet glaciers draining the eastern side of the Greenland Ice Sheet (Fig. 12). This is one of the few glaciers in Greenland having an archival record of flow dynamics from field measurements conducted in the late 1960s. We re-mapped the flow pattern to investigate possible changes in glacier dynamics. In fact, the flow dynamics have remained almost constant over the period between the late 1960s and 2001–2002 (Stearns et al., in press). Future work will apply similar methods to other Greenland glaciers for which archival data exist.

The technique has been applied to Byrd Glacier, which drains one of the largest catchment basins in East Antarctica (~10^6 km^2). To date, very few velocity maps are available for glaciers south of 81° S, the limit of Radarsat interferometric coverage. The Byrd Glacier flows at speeds exceeding 600 m/year in its lower reaches, where it is confined in a fjord that cuts across the Transantarctic Mountains. The flow dynamics of Byrd Glacier were first

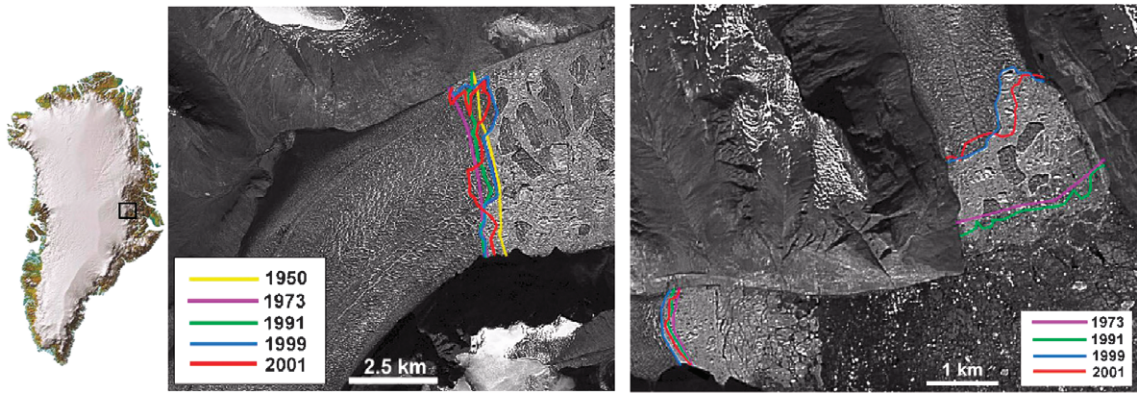

Fig. 12. Tidewater glacier terminus change in East Greenland reconstructed from aerial photography (1950), Landsat MSS (1973), Landsat-5 (1991), Landsat ETM+ (1999) and ASTER (2001, base image) imagery.

described by field surveys of ice motion conducted in 1978 (Brecher, 1982). The flow pattern was updated for an 11-month interval in 2001 using two ASTER images. Subtraction of the second flow map from the first shows that the central trunk of Byrd Glacier has decelerated from ~820 m/year in 1978 to ~650 m/year in 2001 (Fig. 13; Stearns & Hamilton, in press). This change is comparable to decelerations of ice streams draining the Siple Coast of West Antarctica (Joughin et al., 2002). The Siple Coast ice streams are known to be changing rapidly, whereas outlet glaciers draining East Antarctica, such as Byrd Glacier, were previously believed more stable. These results from ASTER add new details to an ongoing community-wide effort to map Antarctic ice sheet dynamics and assess it for mass balance.

3.4. The new Swiss glacier inventory 2000 (SGI2000)

The new inventory of Swiss glaciers is based on Landsat Thematic Mapper (TM) satellite data that have been processed in a GIS environment; lately, ASTER has begun

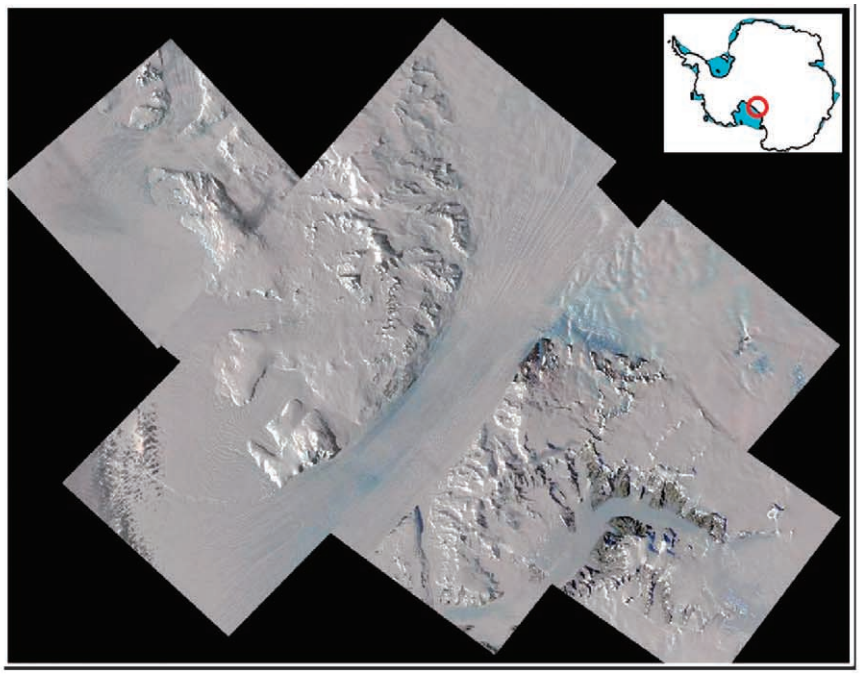

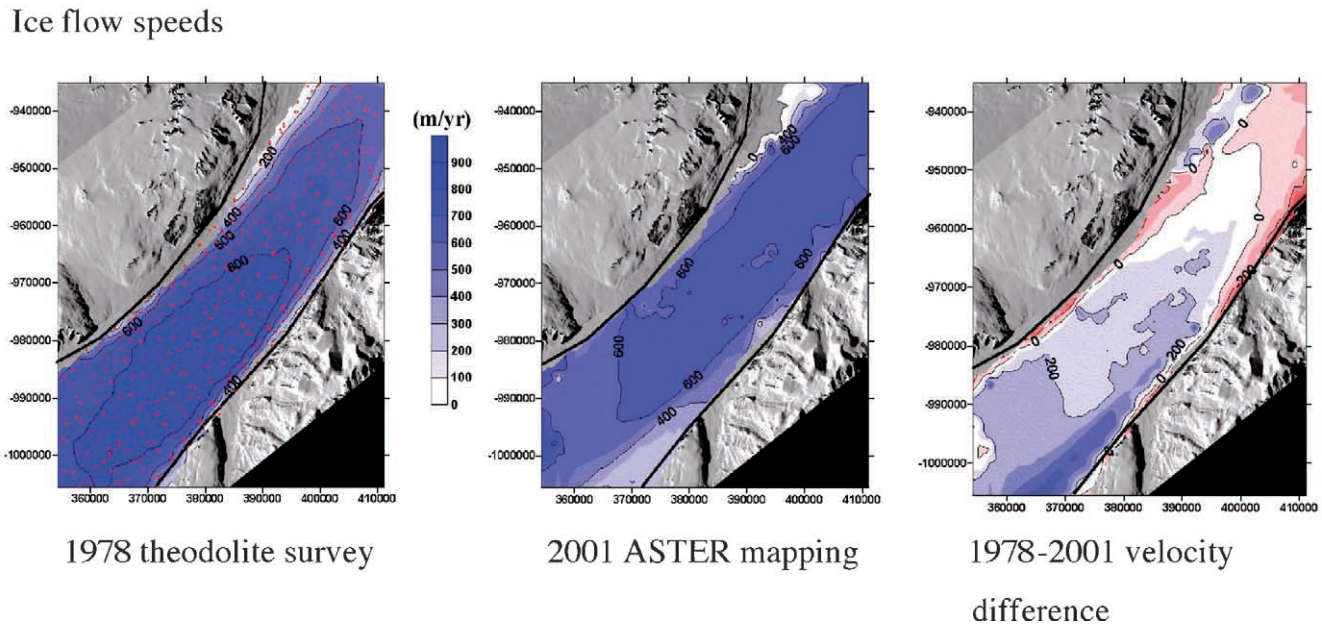

Fig. 13. Byrd Glacier, Antarctica. (top) ASTER image mosaic. (bottom) Surface flow speeds determined by a 1978 theodolite survey (left), and feature tracking in ASTER image analysis using two recent images (center) and the velocity change (right) during two recent time periods (C and D).

to contribute. The very low reflectance of ice and snow in the SWIR part of the spectrum has been utilized for automated mapping of clean glacier ice by means of thresholded TM band 4/TM band 5 ratio images. A digital elevation model and derivatives were combined with the respective glacier outlines to obtain 3D parameters of individual glaciers (Kääb et al., 2002; Paul, 2002). Glacier basins were manually digitized according to the glacier outlines from the former 1973 inventory, which have been digitized from the original topographic maps for this purpose as well (Fig. 14). The methods developed for the SGI2000 also serve as a pilot study for worldwide glacier inventorying within the framework of GLIMS.

The following results are obtained from the specific analysis of glacier changes in Switzerland (Paul et al., in press):

- Swiss glaciers lost ~18% of their 1973 total area until 1998/99, mainly after 1985 (from 1973 to 1985: −1%). This is a seven-fold increased decadal loss rate compared to 1850–1973 (Fig. 15). Small glaciers (<1 km^2) contribute 44% to the total loss of area although they cover only 18% of the total area.
- The relative change in glacier area is highly individual (shrinking and stable glaciers are found side by side) and depends on glacier size with an increasing scatter towards smaller glaciers. This suggests that only a large sample of glaciers will give reliable information of glacier change in a specific region and that the size distribution of any investigated sample should always be given.
- The observed non-uniform changes in glacier geometry (separation from tributaries, increasing areas with rock outcrops, disintegration) indicate massive downwasting in the past two decades in response to changed climate. A further enhancement of such changes is likely due to several positive feedbacks (e.g. additional heating from rock outcrops, more surface melt, decreasing albedo).

The extrapolation of current changes in glacier hypsography (area-elevation distribution) will lead to ice-free regions below 2000 m a.s.l. by 2025, and below 2500 m a.s.l. by 2050.

3.5. Mountain geomorphology and Alpine Valley Glacier classification

Considerable interest concerns the interaction of climate, tectonics, and surface processes in topographic evolution of mountains (Bishop & Shroder, 2004; Molnar & England, 1990; Raymo & Ruddiman, 1992). Mountain geomorphology has focused on surface processes and relief production (Bishop et al., 2003; Burbank et al., 1996; Harbor, 1992; Montgomery, 2004), the magnitude and spatial distribution of uplift and erosion (Gilchrist et al., 1994), and modeling of

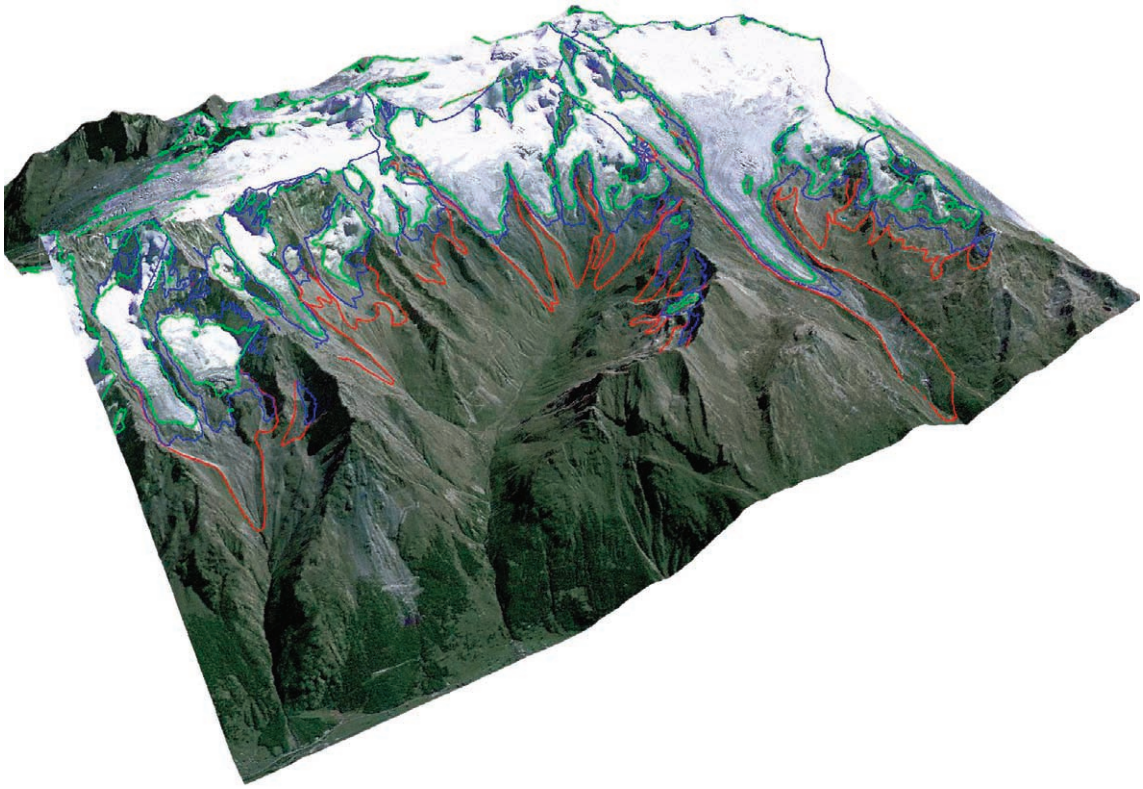

Fig. 14. Synthetic oblique perspective view of Taeschalp (Valais, Switzerland) with a fused IRS/TM image draped over a DEM. Digitized glacier outlines from 1850 and 1973 are shown in red and blue, respectively, TM-derived outlines from 1998 are depicted in green. The large glacier to the upper right is Findelengletscher (16 km^2). DEM © 2004 swisstopo (BA XXX).

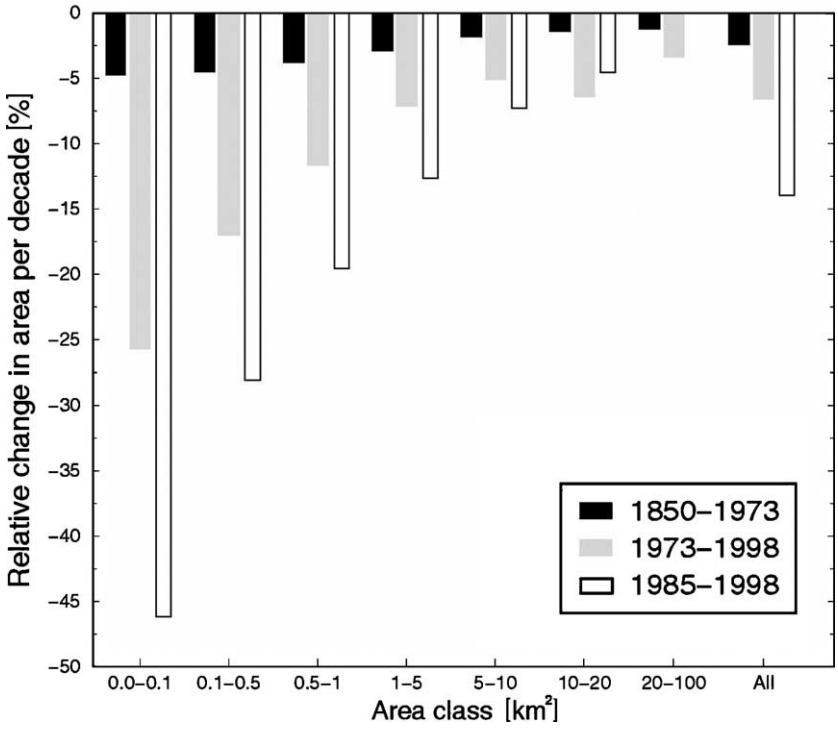

Fig. 15. Relative change in Swiss glacier area per decade for seven size classes and three time periods. The acceleration of glacier wastage since 1985 is remarkable, but the samples used for each period are not the same.

surface processes and geodynamics of orogenesis (MacGregor et al., 2000; Tomkin & Braun, 2002). A climate-forcing hypothesis suggests that radiative and atmospheric forcing regulates glaciation and glacial erosion, which reduces lithospheric mass, thereby causing isostatic, and possibly local tectonic uplift (Molnar & England, 1990). Key issues are spatio-temporal and scale dependencies of topographic variation, climate, and surface processes (Bishop et al., 2003; Bush et al., 2004; Montgomery, 2004).

Glaciers not only generate debris but also are great conveyors of debris to valleys. Satellite remote sensing offers a means to assess spatial variation in glacial debris production and transport rates in alpine regions. Glaciological parametric measurements provided by GLIMS are aiding landscape evolution modeling and are yielding insights into the roles of glaciation in erosional denudation and relief production. GLIMS glacier mapping has revealed high-altitude glacier erosion surfaces throughout the western Himalaya. Cosmogenic exposure-age dating of these surfaces and moraines indicate glacier advances thought to represent monsoon-enhanced glaciation caused by orbital forcing. Paleoclimatic conditions were significantly different than today, which suggests that the landscape is not in topographic equilibrium (erosion and uplift rates are unequal). This explains vastly different denudation rates reported by Shroder and Bishop (2000).

Preliminary glacier erosion simulations with input parameter estimates obtained from ASTER imagery and DEMs depict nonlinear variation in glacial incision rates. These simulations support empirical deductions indicating significant glacial erosional formation of relief (e.g., Bishop et al., 2003).

New insights into glaciers and landscape evolution come from assessing ice velocity fields (the debris-conveyor aspect of glaciers). Kääb et al. (2005) generated DEMs and ice velocity estimates in the Bhutan Himalaya (Fig. 4), which demonstrate significant spatial variability in glacier flow. South-side glaciers exhibit significantly lower velocities (mainly 10–20 m/year), vs. much higher velocities on the north side (20–200/year). This suggests higher basal velocity for the northern glaciers and stagnant ice for the southern ones. This has implications for glacier erosion, as it is generally assumed that glacial abrasion rates are proportional to basal sliding velocity (MacGregor et al., 2000; Tomkin & Braun, 2002).

The overlapping effects of multiple debris-forming glacial processes (e.g., plucking, grinding, subglacial fluvial erosion, and landsliding) make for a complex system. The north–south asymmetry in glacier dynamics evident across Bhutan's Himalaya should produce differential erosion rates, thus explaining differential debris loads on north- and south-side glaciers (Fig. 4). We also expect significant variations in glacial erosion and relief production with altitude and with time during glacial/deglacial cycles (Bishop et al., 2001, 2003). In fact, the debris loads (fractional debris cover) evident on south side glaciers exceed those on north side glaciers, opposite to the pattern expected from recent flow speeds. This condition suggests recent stagnation of south-side glaciers, consistent with the documented growth and aggregation of abundant

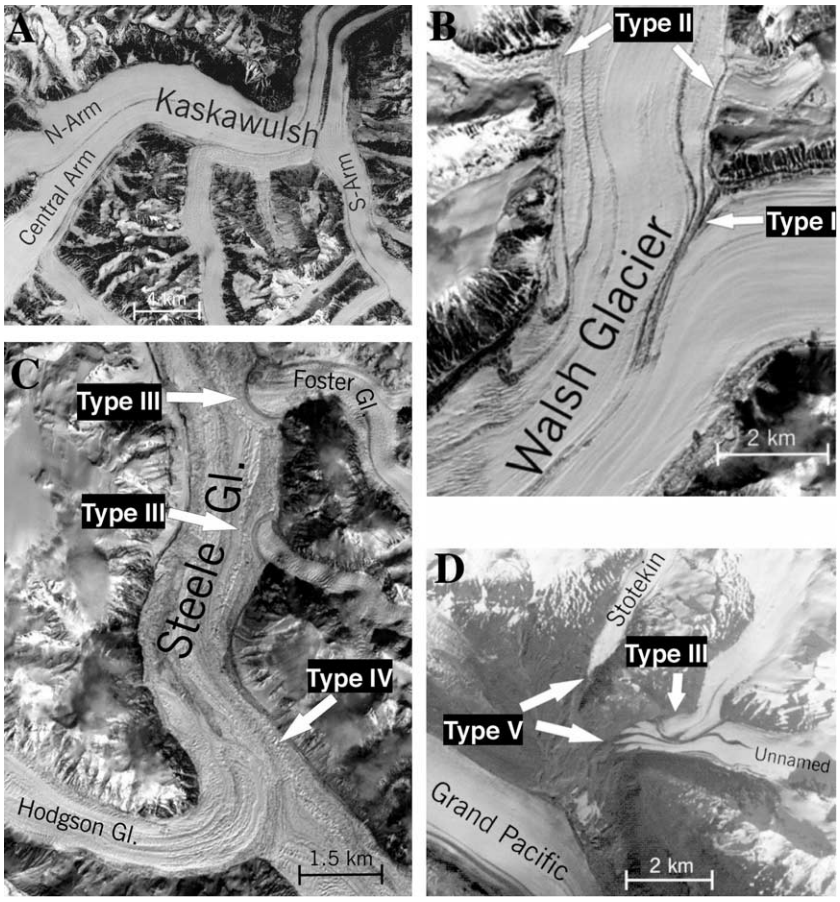

Fig. 16. ASTER imagery illustrating tributary–trunk relations in Yukon Territory glaciers. (A) Kaskawulsh Glacier with coalescing (Type I) tributaries. ASTER image is from 20 May 2003. (B) Sheared off tributaries and tear-shaped looped moraines on Walsh Glacier. ASTER image is from 3 May 2002. (C) Steele Glacier with overriding tributary (Hodgson) and bulging tributaries (Foster and unnamed glacier). ASTER image is from 3 May 2002. (D) Grand Pacific Glacier with detached tributaries (Stotekin and unnamed glacier). Note the bulging tributary on the unnamed glacier. ASTER image is from 4 Oct 2000.

large glacial lakes on south-side glaciers starting in the 1950's.

On the largest scales, glacial-alpine geomorphology is concerned with the integration and form of glacial valleys, which are modifications of antecedent tectonic and fluvial valley structure. Most valley glacier systems are dendritic, where several first, second- and higher-order tributaries flow into trunk glaciers (Fig. 16). For glacierized mountain systems, tributary-trunk relations affect ice flow dynamics, mass balance, and lake formation (e.g. Brecher, 1969; Gudmundsson et al., 1997; Jiskoot et al., 2001). Such interactions, especially oscillations in the relative vigor of ice flow among tributaries and trunks, are mainly responsible for the parallelism, convergence, divergence, or loopiness of medial moraines in the downstream segments of trunk glaciers (Clarke et al., 1986). A common phenomenon in places such as the Chugach Range (Alaska) is the detachment of retreating tributaries from their former trunks and formation of unstable and often dangerous ice-dammed lakes in the gap formed between the detached glaciers (e.g., Van Cleve Lake in Fig. 5). These phenomena are observable by satellite monitoring and in principle are predictable.

The Yukon Territory glacier inventory, based on pre-1980 aerial photographs, was analysed for hierarchy of tributaries and trunks in the St. Elias Mountains (Ommanney, 1980) and now is being updated with analysis of ASTER and ETM+ imagery. A new classification has been developed: 1) Simple tributaries (446 glaciers), 2) Trunks (143 glaciers: e.g. Steele, Dusty, Kaskawulsh glaciers), 3) Tributaries that are also trunks (154 glaciers: e.g. Brabazon, Hodgson, South arm Kaskawulsh), 4) Former tributaries, now detached (125 glaciers: e.g. Stotekin Glacier), and 5) Former tributaries that are still trunks (16 glaciers). There are 884 glaciers in the St. Elias Mountains on which tributary–trunk interactions can be studied. The Yukon glacier inventory also lists 141 former tributaries. Due to continuing glacier recession, more glaciers have detached from their trunks since then and others will soon detach. Grand Pacific Glacier (Fig. 15D) is 55 km long and has three former tributaries listed in the inventory: Stotekin Glacier and an unnamed glacier are shown in Fig. 16D. A comparison of the glacier terminus positions to those on a mid 1980s Landsat 5 MSS image (Clarke & Holdsworth, 2002), reveals that these glaciers have receded ~1.8 km in 20 years.

To aid our work regarding alpine glacier geomorphometry and glacier lake hazard assessment and prediction, we have further developed a classification of tributary–trunk relations on the basis of ice flow activity ratios. Examples of confluence types in the St. Elias Mountains (Yukon Territory) are illustrated with ASTER images (Fig. 16). The type of interactions among tributaries and trunks depends on the following attributes, among others. (1) The tributary–trunk activity ratio, R_a. If $R_a < 1$: trunk flows faster than tributary. If $R_a = 1$: both systems have similar ice flow velocities. If $R_a > 1$: tributary flow faster than trunk. (2) Size ratio. (3) Entrance angle. (4) Entrance slope. (5) Entrance depth. (6) Location of entrance (e.g. above vs. below the equilibrium line, in the compressive vs. extensive flow zone). We have developed the following classification:

Type I: Coalescing flow units ($R_a = 1$)
Type II: Sheared off tributaries ($R_a \ll 1$)
Type III: Bulging tributaries ($R_a > 1$)
Type IV: Overriding tributaries ($R_a \gg 1$)
Type V: Recently detached tributaries

Type I tributaries involve a rough constancy of the relative flow magnitudes of tributary and trunk glaciers. Types III and IV involve dynamic variations in relative flow magnitudes, and Type V involves retreat of the tributary or, less commonly, the trunk.

Examples are found in ASTER images of each of the five classes. Eleven ASTER images, covering most of the above-mentioned 884 glaciers between 4 Oct 2000 and 13 February 2003, were examined for tributary–trunk interactions; the majority is of the coalescing type, where, after joining, the two flow units continue down valley in parallel. Contrasting with those, surge-type glaciers are commonly discerned by looped tear-shaped medial moraines. These moraines are formed when R_a at the confluence changes from >1 to $\ll 1$, as when a tributary bulge is sheared and elongated downstream during a surge of the trunk. Walsh Glacier (Fig. 16B) surged in 1961–1964 (Clarke & Holdsworth, 2002); its two tributaries are a good example of this type of confluence. Steele glacier (Fig. 16C) surged in 1966 and Hodgson Glacier some years later, pushing into Steele and completely overriding it (Clarke & Holdsworth, 2002). Foster glacier (Fig. 16C) is an active tributary of Steele glacier's depleted tongue and is pushing a bulge onto its trunk and forming a striking terminal moraine, as is a smaller tributary just upstream of Foster Glacier. Fig. 10 shows a similar Type III junction in Pakistan and has the satellite image time series necessary to show the recent reconnection of the Liligo Glacier tributary to the Baltoro Glacier. Fig. 16D (Unnamed former tributary of Grand Pacific Glacier) also shows a bulging tributary; the compressive interaction on the trunk is observed as an accordion-type moraine upstream of the confluence. Much can be inferred about recent glacier dynamics from single images using this classification.

3.6. Interpretation of Glacier Lake Dynamics by ASTER Imaging

The exquisite turquoise colors of some glacier lakes (exemplified in Fig. 3H,I), and the absence of these colors in some other glacier lakes (Fig. 5) begs the questions of why this difference exists and whether remote sensing of spectral properties might be used to explore glacier-lake dynamics relevant to glacier lake hazards, such as seasonal and long-term changes in meltwater input and calving. Glacier grinding of rock flour vs. normal fluvial abrasion of grains in a hydraulic medium is key. Rock lithology also influences sediment grain size and lake water quality and color, and so does water depth relative to scattering length scales. Near Peru's glaciers, rock lithology is monotonous andesite and similar rocks, and lake depth is generally much greater than light scattering optical depths except at the edges, and so these are not important variables. Other variables are lake surface wind and wave conditions, sky conditions, and the emission and solar incidence angles, but for a single clear-sky image we assume that these conditions differ little from one lake to another. Lake color differences in our Peru scene (Fig. 3) thus may be explained mainly by differences in (1) turbid meltwater input, (2) the sediment settling time, and (3) lake water residence time.

For each lake and set of circumstances, there is a characteristic grain radius above which grains tend to settle, and below which they remain suspended until discharged through a lake outlet. The critical radius is achieved when settling time (accounting for lake turbulence) equates to the lake water residence time. It is possible to start with the Stokes flow solution to arrive at the variations in critical radius that occur in response to variations of glacier meltwater input. With the simplifying assumption that sediment particle radius distribution and particle number density of the meltwater is constant, but the rate of meltwater input varies, the critical particle radius in a given lake is proportional to the square root of meltwater volume input.

If glacier water influx increases into a lake, the maximum suspended particle size and particle number density will increase, and this affects light scattering, the absorptions due to water and sediment grains, and hence, lake color. As meltwater influx rises, maximum particle radius and particle number density in the lake increase, absorption due to the water decreases, and the scattered/re-emitted light from the lake looks more like light reflected from fresh rock debris. For high turbidities, these lakes are gray (or whatever color the rock detritus is) to the eye. For decreased meltwater input, absorption due to water increases and the preferential red absorption due to water is enhanced, such that scattered light emitted from the lake looks turquoise both to the eye and in our false-color RGB composites. In lakes having no glacial input, lake water is clear, there is almost no scattering or absorption due to

suspended rock particles, light path lengths are long, and almost all visible and infrared wavelengths are absorbed; deep, clear lakes are dark throughout the visible and near/shortwave infrared, and so are black in our RGB false-color composites.

This model explains the rock-like color and albedo of Alaskan glacier lakes, where glaciers are huge, precipitation is high, glacier flow speeds and glacial erosion are rapid, and meltwater throughput and turbidity are high. Thus, the Alaskan lakes look spectrally (Fig. 5B) and visibly (Fig. 5J–M) like freshly crushed moraine rock or debris-covered ice, because there is high glaciological activity. In the case of glacier lakes in Peru (Fig. 3), the glaciers are relatively small and the lakes are turquoise. In sum, variations in glacier/lake interactions (normal seasonal changes and transient dynamical interactions) are manifested in changes in lake color. ASTER data are helping to define instrument parameters that could make practical use of this type of information in hazard assessment.

4. Practical applications and significance for climate change

4.1. Glacier hazards

Glacier and permafrost hazards increasingly threaten human lives, settlements and infrastructure in high mountain regions (Xu & Feng, 1989). Related disasters may kill many people and cause damages or mitigation costs in the order of several hundred million EURO as a longterm worldwide annual average. With dynamic cryospheric responses to changing climate, and with human settlements and activities increasingly extending towards dangerous zones, the hazard situation posed by glaciers and permafrost also is rapidly evolving beyond historical knowledge (Haeberli & Beniston, 1998; Kääb et al., 2005).

Due to difficult site access and the need for fast data acquisition, satellite remote sensing is of crucial importance for high-mountain hazard management and disaster mapping (needed for instance to discern the particular nature or cause of a disaster and to monitor secondary conditions that may develop in the aftermath). ASTER in particular provided assistance for hazard and disaster assessment in a number of cases, e.g., the 20 September 2002 rock/ice avalanche at Kolka–Karmadon, North Ossetian Caucasus, Russia, and the spring 2002 glacier lake on Belvedere glacier, Italian Alps (Kääb et al., 2003b). Imaging opportunities by ASTER are governed at one level by Terra's 16-day nadir-track repeat period, but for emergency situations, the ASTER VNIR sensor can be pointed cross-track, allowing for repeat imaging as frequently as every 2 days. Cross-track pointing is of special value for monitoring dangerous and rapidly developing situations, where ASTER can thus support disaster management (Kääb et al., 2003b).

The following list gives an overview of the most important and typical glacier hazards, where ASTER imagery is able to contribute to the assessment:

- Glaciers and their fluctuations may form lakes whose breakouts cause severe floods and debris flows. For instance, the current massive glacier retreat, prevailing on a global scale, leads to enhanced formation and growth of moraine- and ice-dammed lakes (Ames, 1998; Chikita et al., 1999; Morales, 1969). As described above, ASTER contributes to the detection and monitoring of such lakes (Huggel et al., 2002; Kääb et al., 2003b; Wessels et al., 2002), enables the modelling of related lake outbursts through the combination of ASTER multispectral data with ASTER DEMs (e.g.; Kääb et al., 2003a), and contributes to the monitoring of glaciers that can permit predictions on future formation of glacier lakes.
- Ice break-off from steep glaciers may result in catastrophic ice avalanches, sometimes combined with snow and/or rock avalanches (Morales, 1969). ASTER multispectral data and DEMs support the management of such disasters (Kääb et al., 2003b) or the detection and modeling of related hazard potentials (Salzmann et al., 2004).
- Glacier surges may involve primary hazards through overrunning of infrastructure, subglacial water outbursts connected to surges, or ice avalanches. We note, for instance, that the Alyeska Pipeline and Richardson Highway in Alaska are built on wasted surge deposits and within about a hundred meters of ice-cored moraine from recent glacier surges and advances. Secondary hazards accompanying glacier surges may be, for instance, damming of rivers and lakes, and consequent lake flooding and then down-stream flooding if a glacier dam is breached. Surge-type glaciers and their associated potential hazards may be detected from single scenes by indicators such as looped moraines (Clarke et al., 1986; Copland et al., 2002). With repeat ASTER imagery, glacier surface displacements and surface velocity fields can be measured, areas of disrupted surface debris patterns revealed, and possible hazards can be observed (Kääb et al., 2003b).
- Debutressing and uncovering of steep valley flanks by retreating glaciers significantly affects the stress regime of the slopes, potentially destabilizing them (Kääb, 2002).

The rapid growth of supraglacial and moraine-dammed lakes in the central and eastern Himalaya are linked to disastrous outbursts and potential for future outbursts (Benn et al., 2000; Chikita et al., 1999; Mool, 1995; Richardson & Reynolds, 2000; Xiangsong, 1992; Yamada & Sharma, 1993); we anticipate that this type of hazard will spread increasingly to the western Himalaya, where glacier lakes are beginning to form. Large moraine-dammed lakes and stagnant valley glaciers of the central and eastern Himalaya will eventually stabilize, but debutressing of hanging

glaciers may cause Kolka–Karmadon-like ice avalanches (Kääb et al., 2003a,b) and Peru-style aluviones to become more frequent.

Three-dimensional topography is crucial for understanding high-mountain hazards. DEM generation from the ASTER along-track stereo is thus helpful in glacier hazard assessments. Natural hazards can be computed based on (1) ASTER DEMs, (2) other terrain data sets, such as permafrost distribution and ground-, firn- and ice-temperatures, (3) climatological data sets such as storm frequency and summer high temperature records and future climate-change models, (4) geophysical data sets such as earthquake occurrence, and (5) human geographical datasets such as population and infrastructure distribution.

The assessment of glacier hazards requires systematic and integrative approaches. Presently, the most successful strategy is based on the combination of remote sensing, modelling with Geographical Information Systems (GIS), geophysical soundings and other local field surveys (Kääb et al., 2005). These methods are best structured in a downscaling approach from area-wide first-order assessments for systematically detecting hazard potentials (i.e., the domain of space-borne remote sensing and GIS-techniques) to detailed ground-based or air-borne local investigations in high-risk areas (i.e., the domain of geophysics, surveying, and air-borne and close-range remote sensing) (Huggel et al., 2004; Kääb et al., in press; Salzmann et al., 2004).

In Section 3.6 above, we highlighted ASTER data indicating that variations in the color of glacier lakes are indicators of glacier and meltwater/lake dynamics, such as seasonal calving and changes in meltwater input. If normal seasonal variations can be defined empirically, then other dynamical events could be signaled by temporal changes in lake color or albedo that fall outside the bounds of expected changes. These nonseasonal variations might have significance for understanding hazards and possibly early warning of a consequential dynamical event. ASTER lacks the temporal frequency of imaging necessary to utilize this signal as a warning system, except in emergency mode of operations; MODIS does have the needed frequency, but at far reduced spatial resolution. A possible ASTER/ETM+ follow-on might have both ASTER-like resolution and MODIS-like temporal frequency; if automated onboard or ground-based processing can make a timely and systematic discrimination of "normal" vs. "anomalous" color changes sufficient for the needs of effective hazard warning.

4.2. Climate-change framework for glacier changes

Heterogeneous climate changes and glacier responses are fundamentally related to the patchy distribution of continents, mountains, and ocean basins, which alter the idealized meridional and zonal flows of energy and moisture such as Hadley circulation (Bush et al., 2004; Cubasch et al., 2001; Stainforth et al., 2005). For instance, in maritime Alaska, glaciers have responded in the last half century to the Pacific Decadal Oscillation (PDO, Bond, 2000) and to 2 K of regional winter warming in that period (Stafford et al., 2000). In Peru, decadal variations of glaciers are controlled by the El Niño Southern Oscillation (ENSO), which is partly but incompletely linked to PDO (Bond, 2000). In the central and eastern Himalaya, glaciers are controlled largely by the annual Indian summer monsoon (Mayewski et al., 1980). In Norway, a discrete change in the temporal trend of mass balance occurred in 1988 simultaneously for many glaciers (Kjollmoen et al., 2004); the cause is not known but such a sudden change likely involves oceanic circulation or atmospheric circulation related to ocean dynamics.

In a world of wasting glaciers, Norway is a notable exception to global trends; many glaciers there have exhibited recent advance or thickening, but even there the trends for the last few years have been toward decreased positive mass balance, or a change from positive to negative balance and terminus thinning. Most monitored glaciers in Norway had an equilibrium line altitude *above* the glacier summits in 2003 (Kjollmoen et al., 2004). The high-altitude thickening (with simultaneous thinning and retreat of the terminus documented recently) in some of Norway's glaciers may be due to increased precipitation related to warming sea surface.

The time constants for such regional controls differ, as do glacier responses, which depend on their sizes, hypsometry, slope aspect, and other details. These spatial and temporal variations need to be understood in order to make effective use of satellite-based glacier-change monitoring as a tool in glacier predictions and water management in these areas.

A global ocean/climate model described in Bush and Philander (1999) includes a doubling of atmospheric carbon dioxide. We use model results provided by Bush to illustrate the sharp lateral gradients in climate change that are expected to affect glacier variations over the 21st Century. That particular model and most other GCMs indicate greatest warming in the northern hemisphere, particularly over the interiors of North America and Eurasia (Fig. 17 and Boer et al., 2000; Haywood et al., 1997; Canadian model summarized by MacCracken et al., 2001; most models in Cubasch et al., 2001; two representative models in Stainforth et al., 2005). However, the Hadley model summarized by MacCracken et al. (2001) and the GCM-sensitivity testing reported by Stainforth et al. (2005) highlight possibilities for a future climate at variance with what a majority of GCMs now suggest.

Even where GCMs tend to agree on overall regionalized patterns of climate change, considerable variation in model outcome is indicated, depending on the feedbacks, the model run times, their topographic and spatial resolutions, and other aspects. GCMs are still inadequate for most quantitative work in glaciology. Notably, they do not adequately resolve mountain ranges. This is a major

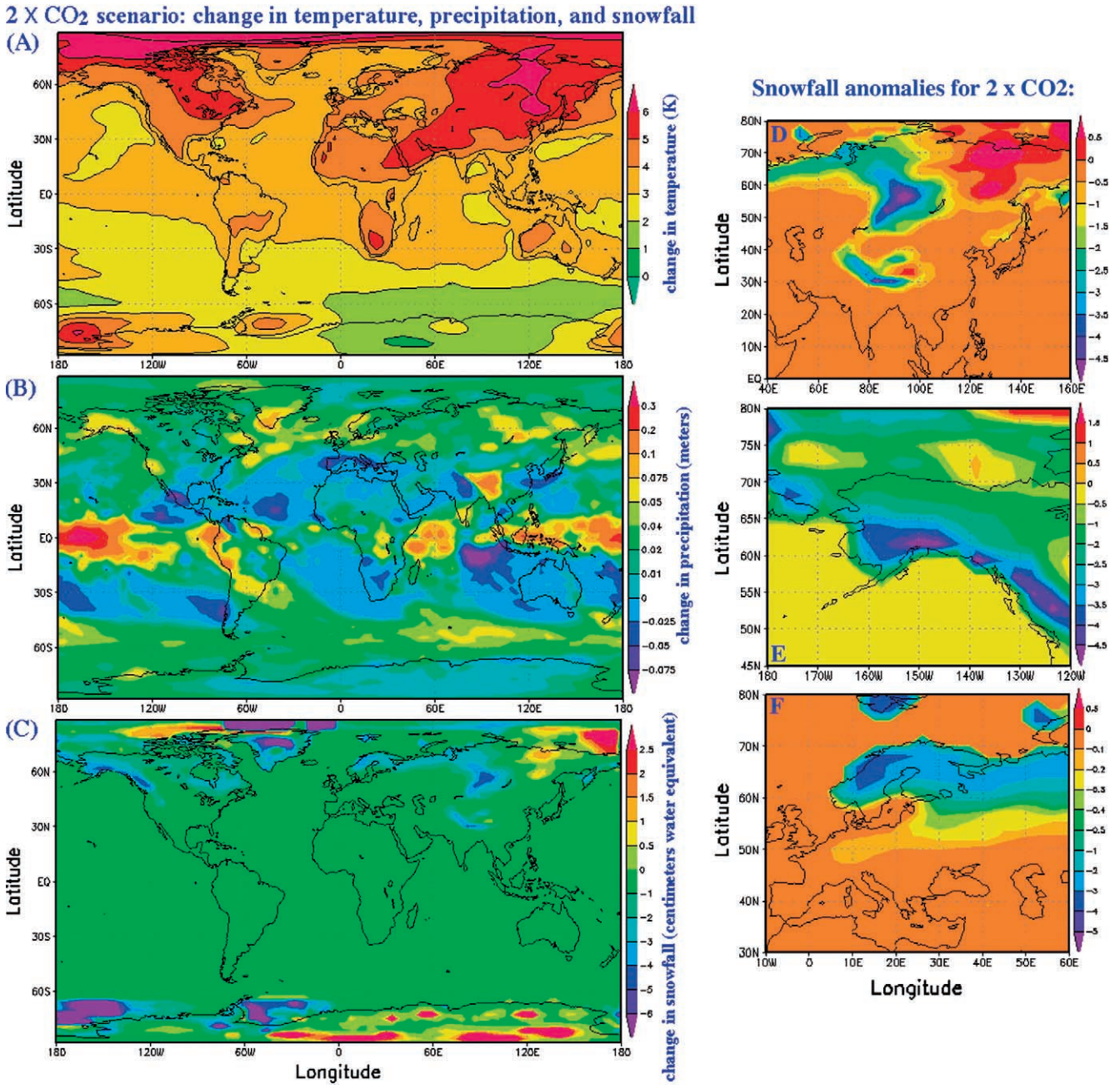

Fig. 17. Global maps of the forecast change of annual mean temperature (A), change in total annual precipitation (B), and change in annual snow accumulation (C) in a 2 × CO_2 scenario, averaged over 69 years of model simulation. (D, E, and F). Change in annual snow accumulation for three regions (Asia, Alaska, and Europe). Units are Kelvins, meters, and centimeters water equivalent for panels (A), (B), and (C), respectively, and also in centimeter for panels (D), (E), and (F). Models due to A. Bush.

handicap. For instance, both the Canadian and Hadley models (MacCracken et al., 2001) show the entire expanse of Washington state to be a comparatively wet region, whereas records show a distinct rain-shadow effect and a bimodal pattern of precipitation due to the Cascades. GCMs lack full resolution of the Cascades (and every other mountain range), and so the homogeneous climate-change signal for that region, as indicated in almost every future-climate GCM, has to be doubted. Since glaciers exist as a balance of snow accumulation and ablation, one cannot use the quantitative output of widely used current GCMs to compute glacier mass balance. However, general trends of increasing or decreasing mass balance may be ascertained qualitatively based on the sign of precipitation and temperature anomalies in these models, with due recognition of the models' limits.

Fig. 18 illustrates qualitative changes to glaciers observed in recent times and projected for the 21st Century. This figure is not quantitative; it is a working hypothesis meant to frame discussion points and to help

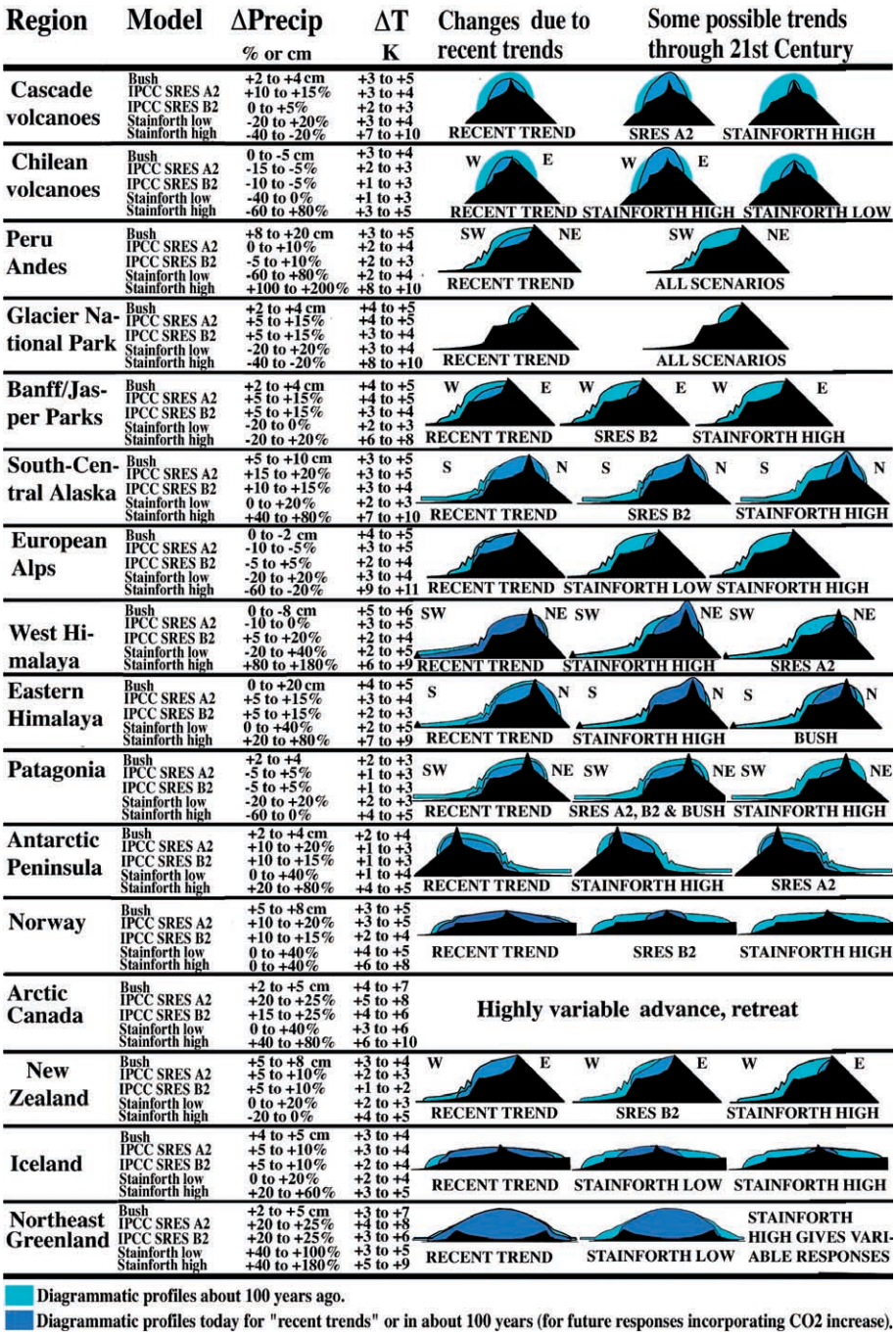

Fig. 18. Summary of five varied climate-change scenarios for models involving increased atmospheric greenhouse gases and changes in other radiative forcings, and diagrammatic illustrations suggesting possible future impacts on glaciers. The reference sources are cited cryptically and limitations of climate models are described in the text.

define desired parameters for future GCMs that will enable viable quantitative glaciological applications. The tabular data in Fig. 18 includes results from Andrew Bush, two fairly mainstream models from the IPCC 2001 report (Cubasch et al., 2001), and two models representing some of the wide model variance modeled by Stainforth et al. (2005). The results for the Bush and Stainforth et al. models are for doubling of CO_2, which is likely to occur well before the end of the 21st Century, whereas the IPCC models are comparisons of late 21st and late 20th Century climate under different CO_2-emissions scenarios.

The diagrammatic glacier responses in Fig. 18 are educated guesses based on each climate model; the trends do not consider quantitatively the relative sensitivity of glaciers to changes in precipitation; in fact this relative sensitivity varies widely: cold-based polar glaciers are highly sensitive to changes in precipitation, but not very

sensitive to temperature (except as affects precipitation); temperate glaciers, especially those having long, low-sloping valley segments such as in Bhutan, are highly sensitive to both types of changes, where even 1 K difference can rapidly stabilize or destroy the valley segments.

In some regions (such as in the Chilean Andes and the European Alps), warming and drying will take place together, according to almost every GCM of 21st Century climate; the clear implication is for continued rapid retreat and disappearance of glaciers in those regions. In other regions, there is a fair consensus that increased precipitation will attend warming (such as in the Canadian Arctic and Iceland); the significance for glaciers is obscured by the opposing signs of the glaciological impacts of those parametric changes.

We take the Himalayan region as an example emphasizing the complexity and uncertainty of coupled ocean/climate/glacier systems. Pleistocene and Holocene glacial oscillations have tended to be synchronous throughout the Himalaya, driven by global insolation, the Indian monsoon, and even North Atlantic circulation, but they are asynchronous with respect to glaciations elsewhere (Anderson et al., 2002; Finkel et al., 2002; Gillespie & Molnar, 1995; Phillips et al., 2000). On the sub-century scale relevant to global warming and human policy and planning, we expect some asynchroneity and nonuniformity of Himalayan glacial retreat.

The Himalaya show strong east–west and north–south variations in glacier response to climate change. Glaciers in central Nepal's Himalaya are retreating or downwasting (Fig. 6) and many glaciers there are undergoing massive lake formation. Similar and more drastic responses are occurring in Bhutan (Fig. 4). Rapid wasting also has been documented since the late 1970s in the nearby Pamir, according to analysis of ASTER imagery and previous data (Khromova et al., 2003). By contrast, many glaciers in the western Himalaya and in Afghanistan's Hindu Kush—including some that exist below the climatic snowline and exist only for windblow, avalanches, and heavy debris cover—are changing surprisingly slowly and may have almost stable termini, and one glacier has even advanced recently (Figs. 8–10). Glaciers on the south side of the eastern Himalaya are in rapid retreat or are undergoing stagnation and in situ disintegration (Fig. 4). Glaciers on the north side of the same parts of the eastern Himalaya are retreating but generally not stagnating or disintegrating (Fig. 4) (Kääb, 2005).

The north–south asymmetry and east–west variations of glacier activity can be explained by (1) snow shadow effects, (2) variations of changes in the fraction of precipitation received as rain and glacier sensitivity to this fraction; (3) east-to-west and south-to-north decreases in monsoonal intensity, and (4) longer glacier dynamical response times of the colder continental glaciers on the continental interior side vs. south-side maritime glaciers. The last few decades of rapid climate change may be felt strongly first—probably already—on south-side glaciers having fastest dynamical response times. Lagging responses of north-side glaciers will eventually catch up. Almost every GCM shows large regional north–south and east–west gradients in predicted warming and precipitation changes across the Himalayan/Central Asian region, and thus suggest that future glacier responses will continue to be highly heterogeneous, even though details of predictable changes depend on the model. The divergence of model predictions is exemplified by the western Himalaya and Hindu Kush region of Kashmir, Pakistan, and Afghanistan: (1) some models predict drying, and others predict a high increase of precipitation; (2) these models differ by a factor of three in the amount of warming that may take place in the next century.

These examples highlight a need to measure and model glacier variations between and within each mountain range, and to run models both backward and forward in time and then compare with the glacier record. However, current GCMs barely resolve mountain ranges. The Bush and Philander model (Fig. 17), for instance, has a grid-cell spacing of about 3.75° longitude by 2° latitude (400×200 km roughly). The spatial variability of predicted snow and precipitation change must be understood more clearly if we are to preserve existing freshwater resources, or at least understand how they are apt to change. Vigilant glaciological, hydrological, and climatological observational networks and numerical model simulations of these coupled components of the Earth system, with improved resolution of mountain ranges, are required.

5. Conclusions and recommendations

Our treatment here includes case studies selected globally, with summaries of more comprehensive results for a couple small regions. This paper does not offer a scientific global sample, and not even a representative sampling of GLIMS data. It is just a sampling of results designed to demonstrate applications of ASTER and other multispectral imagery to make glaciological measurements and show that glacier changes are extremely varied. A more thorough examination of glacier changes will be presented in stages in the future.

Due to accelerating emissions of CO_2 and some other greenhouse gases, the 21st Century's climate changes are likely to impact some glacierized regions more strongly than others and more strongly overall than 20th Century climate changes already have (Albritton et al., 2001; Cubasch et al., 2001). However, individual glacier responses seen by remote sensing are commonly not readily attributed to a specific cause, such as climate change, because of (1) flow instabilities caused by the non-

Newtonian rheology of ice and subglacial till and the stick-slip nature of glacier sliding (Bindschadler et al., 2003; Kamb, 1991; Wang & Warner, 1998); (2) the complex pattern of heterogeneous climate perturbations (Bamber et al., 2004; Stainforth et al., 2005); (3) nonuniform time scales of glacier responses to perturbations and asynchroneity of responses (Baisheng et al., 2003; Gillespie & Molnar, 1995); and (4) special processes that affect accumulation, deformation, or ablation (Bindschadler et al., 2003; Copland et al., 2002; De Angelis & Skvarca, 2003; Dowdeswell & Benham, 2003). Not all of these aspects can be discerned by remote sensing, and rarely can the change of an individual glacier be attributed to one cause. For instance, the Gangotri (Fig. 6A) has exhibited a quarter millennium of accelerating retreat ideally interpreted as due to accelerating warming, but we cannot be certain. The retreat trend of the Gangotri Glacier is seemingly inconsistent with a lagging response to the end of the Little Ice Age, which would instead produce slowing retreat. The cause of the retreat (or advance) trend of any individual glacier must be considered along with multiple potential causes. However, statistics on large numbers of glaciers can see through complexity to the climate signal.

To take another example of complexity, the rapid retreat of the calving terminus of Miles Glacier (Alaska) over the last century and smaller changes this century (Fig. 5) may be related to climate change, which is generally causing accelerating retreat in the region. The slowdown of retreat of the Miles Glacier is probably a response to reduced interaction with the Copper River into which the glacier flows.

We have highlighted additional examples that point out the inadequacy of measuring only length or area changes. Rather, GLIMS must also move toward morphometric analysis of glacier surfaces in addition to length and area. Use of multispectral remote sensing methods in glacier-change assessment is restricted by a limited capability to discern changes in glacier thickness, which in individual cases can dominate mass balance. For example, field measurements and models show that the terminus of the Khumbu Glacier is accumulating a thickening, insulating debris blanket on thinning ice dammed up behind (but not retreating significantly from) a high end moraine (Kadota et al., 2000; Naito et al., 2000). Satellite imaging shows that the termini of the Khumbu and nearby Rongbuk Glaciers have undergone almost no change in terminus position (Fig. 6), but this does not mean that these glaciers are stable. ASTER and similar imaging systems can contribute to assessment of evolution of glacier surfaces, because lakes, pits, transient snowlines, debris cover, and other features are visible and measurable. GLIMS requires the development of the tools needed to make quantitative characterization of glacier surfaces as well as outlines, even if we normally cannot make direct measurements of mass balance by remote sensing.

Some instances of advancing glaciers, such as the Lilago (Fig. 10), might be confusing or misleading if interpreted in terms of a direct response to regional climate change. If the advance is due to a climatic forcing, rather than due to a chaotic or oscillatory dynamical instability, it may be due to increased generation of meltwater and hydraulic pressurization and sliding at the bed (and so might lengthen and thin even as it loses mass), or it might be due to locally increased precipitation and positive balance. Whether a quarter-century advance qualifies as a surge is not clear, but it may be an oscillatory change. Glacier surges result in natural cycles of rapid advance and slow retreat and stagnation (conversely, tidewater glaciers and floating tongues commonly exhibit slow advance and sudden breakup).

Only a systematic glaciological measurement approach (using remote sensing and available field data) can resolve climatological and other causes of glacier change sufficient for prediction. Large statistics are needed to average out dynamical oscillations and other instabilities, transient behaviors, effects due to microclimates, and other "anomalies." In regions where GLIMS and others have completed some level of a systematic image analysis and glacier measurement program using available remote sensing and field data (e.g., Figs. 11, 14, and 15), there is no question that retreat is widespread and dominant.

A global trend of retreating, wasting, and disappearing glaciers is glaciology's biggest story. It is not the whole story. Reading the whole story and understanding practical impacts of changing glaciers on water resources and hazards will require intensive glacier monitoring and improving our understanding of the links between climate and glacier responses on the level of whole regions and individual important glaciers. As GLIMS moves toward more systematic assessment of glacier variations, we expect to be able to address some critical global and regional questions (Fig. 1B). How does the global pattern of recent glacier change relate to global models of future climate? Will glacier trends accelerate? Will the pattern of responses shift? How will these changes affect economic development and ecosystem integrity? We can make educated guesses but cannot make specific and reliable predictions without more detailed GCMs, coupling of GCMs to glacier dynamical models, and close comparison of the models with recent climate records and recent glacier changes. This is where GLIMS is going.

Fig. 18 encapsulates a working hypothesis that we hope will help motivate global integration of improved climate and glacier models and observations. That objective will require merging of climate models having improved spatial resolution over mountains with glacier dynamical models that include conventional ice physics and realistic processes involving bed and meltwater dynamics. It will require a consideration of uncertainties in measurements of glacier variations as a function of time with a range of

climate models that represent uncertainties in those models. Due to computing limits, current GCMs have a grid-cell spacing much coarser than individual glaciers; major mountain ranges are barely resolved and are severely smoothed. This impacts the applicability of GCMs to individual glaciers and mountain ranges. To compensate, climate modelers must move toward variable-grid spacings in nested GCMs to catch glaciologically critical details over mountain ranges. Resolution in GCMs of large Arctic ice caps and large mountain glaciers such as the Malaspina and Bering is conceivable, and then glacier dynamics models can be coupled. Coupled glacier-climate models have a strong capacity to test the climate results by running the models to past lower levels of greenhouse gases, and then to use successful GCMs (those explaining recent observed glacier fluctuations) with glacier dynamics models to make improved projections of future glacier variations.

Accelerating climate changes expected throughout this century will have dramatic implications for glaciers and for the people and ecosystems dependent on them or surviving in spite of them. The effects will be heterogeneous and not always in accord with simple expectations or recent past behavior. Arid regions dependent on glacierized mountains for freshwater, for instance western China, Uzbekistan, Afghanistan, Kyrgyzstan, and Pakistan, may be particularly prone to environmental, economic, and political upheavals due to glacier recession (Froebrich & Kayumov, 2004; Fukushima et al., 1991; Hewitt, 1961; Micklin, 2004; Romanovsky, 2002; Shiyin et al., 2003; Yang & Hu, 1992). Other areas may benefit in the short-term if meltwater resources increase as glaciers melt. The glaciology community carries an obligation to improve our predictions of these changes and to assist society in building defenses against these changes or in taking cooperative advantage of them.

Because glacier vigor depends upon cloudiness and precipitation as well as temperature, the growth or shrinkage of glaciers has a complex relation to climate change, as our examples suggest. The changes for a large number of glaciers now being quantified through GLIMS, especially in relation to historic records, confirm and support the general recessional trend and its relation to global warming as documented in earlier studies with a modest number of glaciers (e.g., Oerlemans, 2005). The challenge facing glaciologists, climatologists, and policy makers is to gain understanding of the regional relation of glacier change to climate adequate to enable confident prediction of consequences to the environment and society.

Acknowledgments

We extend our gratitude to the Japanese and American ASTER mission operations and engineering staffs for making this work possible. Paul Geissler, Alan Gillespie, and anonymous readers provided helpful reviews. H. Jiskoot thanks Glen Hendrickson for help with the inventory and image data, and Jeffrey Schmok for the copy of GLADYS, the Yukon Territory glacier inventory. Jiskoot's research on tributary–trunk interactions is funded through an NSERC Discovery Grant. A. Kääb and F. Paul thank Max Maisch, Tobias Kellenberger, and Wilfried Haeberli for assistance and guidance; their work has been funded by the Swiss National Science Foundation (21-54073.98). We thank Jim Torson, David Gaseau, Trent Hare, and Syed Iqbal Hasnain for assistance on various aspects. The U.S. authors were supported by NASA grants through NASA OES-02 and OES-03. GLIMS at NSIDC is supported by NASA awards NNG04GF51A and NNG04GM09G.

References

Abdalati, W., & Steffen, K. (2001). Greenland ice sheet melt extent: 1979–1999. *Journal of Geophysical Research*, *106*(D24), 33,983–33,989.

Abdalati, W., et al. (2001). Outlet glacier and margin elevation changes: Near coastal thinning of the Greenland ice sheet. *Journal of Geophysical Research*, *106*(D24?), 33,729–33,741.

Albritton, D. L., et al. (2001). Technical summary. In J. T. Houghton (Eds.), *Climate change 2001: The science of climate change* (pp. 21–83). Cambridge University Press.

Ames, A. (1998). A documentation of glacier tongue variations and lake development in the Cordillera Blanca, Perú. *Zeitschrift Für Gletscherkunde und Glazialgeologie*, *34*, 1–36.

Anderson, D. M., Overpeck, J. T., & Gupta, A. K. (2002). Increase in the Asian southwest monsoon during the past four centuries. *Science*, *297*, 596–599.

Bahr, D. B. (1997a). Global distributions of glacier properties: A stochastic scaling paradigm. *Water Resources Research*, *33*(7), 1669–1679.

Bahr, D. B. (1997b). Width and length scaling of glaciers. *Journal of Glaciology*, *43*(128), 557–562.

Baisheng, Y., Yongjian, D., Fengjing, L., & Caohai, L. (2003). Responses of various-sized alpine glaciers and runoff to climatic change. *Journal of Glaciology*, *49*, 1–7.

Bamber, J. L., Krabill, W. B., Raper, V., & Dowdeswell, J. A. (2004). Anomalous growth of part of a large Arctic ice cap: Austfonna, Svalbard. *Geophysical Research Letters*, *31*, L12402, doi:10.1029/2004Gl019667.

Bamber, J. L., & Rignot, E. (2002). Unsteady flow inferred for Thwaites Glacier, and comparison with Pine Island Glacier, West Antarctica. *Journal of Glaciology*, *48*, 237–246.

Benn, D. I., Wiseman, S., & Warren, C. R. (2000). Rapid growth of a supraglacial lake, Ngozumpa Glacier, Khumbu Himal, Nepal. *International Association of Hydrological Sciences Publication*, *264*, 177–185.

Bennat, H., Heidrich, H., Grimm, J., Sievers, J., Walter, H., & Wiedemann, A. (1998). Das "Geowissenschaftliche Informationssystem Antarktis" (GIA) am Institut für Angewandte Geodäsie (IfAG). *Petermanns Geographische Mitteilungen*, *287*, 13–34.

Berthier, E., Arnaud, Y., Baratoux, D., Vincent, C., & Remy, F. (2004). Recent rapid thinning of the "Mer de Glace" glacier derived from satellite optical images. *Geophysical Research Letters*, *31*(17), L17401.

Berthier, E., Raup, B., & Scambos, T. (2003). New velocity map and mass-balance estimate of Mertz Glacier, East Antarctica, derived from Landsat sequential imagery. *Journal of Glaciology*, *49*, 503–511.

Bindschadler, R. A., & Bentley, C. R. (2002). On thin ice? *Scientific American*, *287*(6), 98–105.

Bindschadler, R., & Vornberger, P. (1998). Changes in the west Antarctic ice sheet since 1963 from declassified satellite photography. *Science*, *279*, 689–692.

Bindschadler, R. A., King, M. A., Alley, R. B., Anandakrishnan, S., & Padman, L. (2003). Tidally controlled stick-slip discharge of a west Antarctic ice stream. *Science*, *301*, 1087–1089.

Bishop, M. P., Bonk, R., Kamp, U., & Shroder Jr., J. F. (2001). Terrain analysis and data modeling for alpine glacier mapping. *Polar Geography*, *25*(3), 182–201.

Bishop, M. P., Olsenholler, J. A., Shroder Jr., J. F., Berry, R. G., Raup, B. H., & Bush, A. B. G., et al. (2004). Global land ice measurements from space (GLIMS): Remote sensing and GIS investigations of the Earth's cryosphere. *Geocarto International*, *19*, 57–84.

Bishop Jr., M. P., & Shroder Jr., J. F., (Eds.) (2004) *Geographic information science and mountain geomorphology.* Chichester: Springer-Praxis.

Bishop, M. P., Shroder Jr., J. F., & Colby, J. D. (2003). Remote sensing and geomorphometry for studying relief production in high mountains. *Geomorphology*, *55*, 345–361.

Bishop, M. P., Shroder Jr., J. F., & Hickman, B. L. (1999). SPOT panchromatic imagery and neural networks for information extraction in a complex mountain environment. *Geocarto International*, *14*, 17–26.

Bishop, M. P., Shroder Jr., J. F., Hickman, B. L., & Copland, L. (1998). Scale-dependent analysis of satellite imagery for characterization of glacier surfaces in the Karakoram Himalaya. Special volume on "remote sensing in geomorphology". In S. Walsh, & D. Butler (Eds.), *Geomorphology*, *vol. 21* (pp. 217–232).

Bishop, M. P., Shroder, J. F., & Ward Jr., J. L. (1995). SPOT multispectral analysis for producing supraglacial debris-load estimates for Batura Glacier, Pakistan. *Geocerto International*, *10*, 81–90.

Boer, G. J., Flato, G., Reader, M. C., & Ramsden, D. (2000). A transient climate change simulation with greenhouse gas and aerosol forcing: Experimental design and comparison with the instrumental record for the twentieth century. *Climate Dynamics*, *16*, 405–425.

Bond, N. A. (2000). The Pacific Decadal Oscillation, air–sea interaction and central North Pacific winter atmospheric regimes. *Geophysical Research Letters*, *27*(5), 731–734.

Braslau, D., & Bussom, D. E. (1978). A glacier inventory method using Landsat MSS CCT. In D. C. Rundquist (Ed.), *The use of Landsat digital information for assessing glacier inventory parameters; an evaluation: Final report, project sponsored by Temporary Technical Secretariat for World Glacier Inventory, International Commission of Snow and Ice, and United Nations Educational, Scientific and Cultural Organization* (pp. 23–40).

Brecher, H. H. (1969). Surface velocity measurements on the Kaskawulsh Glacier. In H. H. Bushnell, & Ragle (Eds.), *Icefield ranger research project: Scientific results 1, Montreal, Quebec* (pp. 127–143). AINA, New York: American Geographical Society.

Brecher, H. H. (1982). Photographic determination of surface velocities and elevations on Byrd Glacier. *Antarctic Journal of the United States*, *17*(5), 79–81.

Burbank, D., Leland, J., Fielding, E., Anderson, R. S., Brozovic, N., Reid, M. R., et al. (1996). Bedrock incision, rock uplift and threshold hillslopes in the northwestern Himalaya. *Nature*, *379*, 505–510.

Bush, A. B. G., & Philander, S. G. H. (1999). The climate of the Last Glacial Maximum: Results from a coupled atmosphere–ocean general circulation model. *Journal of Geophysical Research*, *104*, 24,509–24,525.

Bush, A. B. G., Prentice, M. L., Bishop, M. P., & Shroder Jr., J. F. (2004). Modeling global and regional climate systems: Climate forcing and topography. In M. P. Bishop, & J. F. Shroder Jr. (Eds.), *Geographic information science and mountain geomorphology* (pp. 403–424). Chichester: Springer-Praxis.

Chikita, K., Jha, J., & Yamada, T. (1999). Hydrodynamics of supraglacial lake and its effect on the basin expansion: Tsho Rolpa, Rolwaling Valley, Nepal Himalaya. *Arctic Antarctic Alpine Research*, *31*, 58–70.

Church, J., Gregory, J. M., Huybrechts, P., Kuhn, M., Lambeck, K., Nhuan, M. T., et al. (2001). Changes in sea level, in climate change 2001. In Houghton J., et al., (Eds.), *The scientific basis: Contribution of Working Group I to the Third Assessment Report of the Intergovernmental Panel on Climate Change* (pp. 639–693). New York: Cambridge Univ. Press.

Clarke, G. K. C., & Holdsworth, G. (2002). Glaciers of the St Elias Mountains. In Williams & Ferrigno (Eds.). Satellite image atlas of glaciers of the world: North America. USGS Professional Paper, *vol. 1386-J* (pp. 301–328).

Clarke, G. K. C., Schmok, J. P., Ommanney, C. S. L., & Collins, S. G. (1986). Characteristics of surge-type glaciers. *Journal of Geophysical Research*, *91*(B7), 7165–7180.

Copland, L., Sharp, M., & Dowdeswell, J. (2002). The distribution and flow characteristics of surge-type glaciers in the Canadian High Arctic. *Annals of Glaciology*, *36*, 73–81.

Cubasch, U., Meehl, G. A., Boer, G. J., Stouffer, R. J., Dix, M., Noda A., et al. (2001). In J. T. Houghton (Eds.), *Climate change 2001: The science of climate change* (pp. 527–582). Cambridge University Press.

De Angelis, H., & Skvarca, P. (2003). Glacier surge after ice shelf collapse. *Science*, *299*(5612), 1560–1562.

de Grancy, & Kostka (1978). *Grosser Pamir. Akademische Druck–u,,.* Graz, Austria: Verlagsanstalt. 399 pp.

Dowdeswell, J. A., & Benham, T. J. (2003). A surge of Perseibreen, Svalbard, examined using aerial photography and ASTER high-resolution satellite imagery. *Polar Research*, *22*(2), 373–383.

Dyurgerov, M. B., & Meier, M. (1997). Mass balance of mountain and subpolar glaciers: A new global assessment for 1961–1990. *Arctic and Alpine Research*, *29*, 379–391.

Dyurgerov, M. B., & Meier, M. F. (2000). Twentieth Century climate change: Evidence from small glaciers. *Proceedings of the National Academy of the United States of America*, *97*, 1406–1411.

Ferrigno, J.G., Mullins, J.L., Stapleton, J., Chavez Jr., P.S., Velasco, M.G., Williams Jr., R.S., Delinski Jr., G.F., et al. (1996). Satellite image map of Antarctica, USGS miscellaneous investigations series, Map I-2560.

Ferrigno, J. G., Williams Jr., R. S., Rosanova, C. E., Lucchitta, B. K., & Swithinbank, C. (1997). Analysis of coastal change in Marie Byrd Land and Ellsworth Land, West Antarctica, using Landsat imagery. *Journal of Glaciology*, *27*, 33–40.

Finkel, R. C., Owen, L. A., Barnard, P. L., & Caffee, M. W. (2002). Beryllium-10 dating of Mount Everest moraines indicates a strong monsoon influence and glacial synchroneity throughout the Himalaya. *Geology*, *31*(6), 561–564.

Frezzotti, M., Capra, A., & Vittuari, L. (1998). Comparison between glacier ice velocities inferred from GPS and sequential satellite images. *Annals of Glaciology*, *27*, 54–60.

Froebrich, J., & Kayumov, O. (2004). Water management aspects of Amu Darya. In J. J.C.J., P. O. Zavialov, & P. P. Micklin (Eds.), Dying and dead seas: Climatic versus anthropic causes. *NATO Science Series* (pp. 49–76). Boston: Kluwer Academic Publishers.

Fukushima, Y., Watanabe, O., & Higuchi, K. (1991). Estimation of streamflow change by global warming in a glacier-covered high mountain area of the Nepal Himalaya. In H. Bergmann, H. P. Lang, W. Frey, D. Issler, & B. Salm (Eds.), International symposium snow, hydrology and forests in high alpine areas Vienna, 11–24 August 1991. *Proceedings. International association of hydrological sciences. IAHS/AISH Publication*, *vol. 205* (pp. 181–188).

Gilbert, O., Jamieson, D., Lister, H., & Pendington, A. (1969). Regime of an Afghan glacier. *Journal of Glaciology*, *8*, 51–65.

Gilchrist, A. R., Summerfield, M. A., & Cockburn, H. A. P. (1994). Landscape dissection, isostatic uplift, and the morphologic development of orogens. *Geology*, *22*, 963–966.

Gillespie, A. R., & Molnar, P. (1995). Asynchronism of maximum advances of mountain and continental glaciations. *Reviews of Geophysics*, *33*, 311–364.

Gregory, J. M., & Oerlemans, J. (1998). Simulated future sea-level rise due to glacier melt based on regionally and seasonally resolved temperature changes. *Nature*, *391*, 474–476.

Gudmundsson, G. H., Iken, A., & Funk, M. (1997). Measurements of ice deformation at the confluence area of Unteraargletscher, Bernese Alps, Switzerland. *Journal of Glaciology*, *43*(145), 548–556.

Haeberli, W., & Beniston, M. (1998). Climate change and its impacts on glaciers and permafrost in the Alps. *AMBIO*, *27*(4), 258–265.

Haeberli, W. R., Frauenfelder, R., Hoelzle, M., & Maisch, M. (1999). On rates and acceleration trends of global glacier mass changes. *Geografiska Annaler. Series A. Physical Geography*, *81A*, 585–595.

Haeberli, W., Hoelzle, M., Suter, S., (Eds.) (1998). Into the second century of world glacier monitoring—prospects and strategies. *Paris: Studies and reports in hydrology*, *vol. 56*. (p. 227). UNESCO Publishing.

Hall, D. K., Bahr, K. J., Shoener, W., Bindschadler, R. A., & Chien, J. Y. L. (2003). Consideration of the errors inherent in mapping historical glacier positions in Austria from the ground and space. *Remote Sensing of Environment*, *86*, 566–577.

Harbor, J. M. (1992). On the mathematical description of glaciated valley cross sections. *Earth Surface Processes and Landforms*, *17*, 477–485.

Hastenrath, S., & Ames, A. (1995). Recession of Yanamarey Glacier in Cordillera Blanca, Perú, during the 20th century. *Journal of Glaciology*, *41*, 191–196.

Haywood, J. M., Stouffer, R. J., Wetherald, R. T., Manabe, S., & Ramaswamy, V. (1997). Transient response of a coupled model to estimated changes in greenhouse gas and sulfate concentrations. *Geophysical Research Letters*, *24*, 1335–1338.

Hewitt, K. (1961). Glaciers and the Indus. *Indus*, *2*, 4–14.

Horvath, E. (1975). In W. O. Field (Ed.), *Glaciers of the Hindu Kush in Mountain Glaciers of the Northern Hemisphere*, *vol. 1*. (pp. 361–409). Hanover, NH: CRREL.

Huggel, C., Kääb, A., Haeberli, W., Teysseire, P., & Paul, F. (2002). Satellite and aerial imagery for analysing high mountain lake hazards. *Canadian Geotechnical Journal*, *39*(2), 316–330.

Huggel, C., Kääb, A., & Salzmann, N. (2004). GIS-based modeling of glacial hazards and their interactions using Landsat TM and Ikonos imagery. *Norwegian Journal of Geography*, *58*, 61–73.

Huybrechts, P. (2002). Sea-level changes at the LGM from ice-dynamic reconstructions of the Greenland and Antarctic ice sheets during the glacial cycles. *Quaternary Science Reviews*, *21*, 203–231.

Jiskoot, H., Pedersen, A. K., & Murray, T. (2001). Multi-model photogrammetric analysis of the 1990s surge of Sortebræ, East Greenland. *Journal of Glaciology*, *47*(159), 677–687.

Jóhannesson, T. (1985). The response time of glaciers in Iceland to changes in climate. *Annals of Glaciology*, *8*, 100–101.

Joughin, I., Abdalati, W., & Fahnestock, M. (2004). Large fluctuations in speed on Greenland's Jakobshavn Isbrae Glacier. *Nature*, *432*, 608–610.

Joughin, I., Tulaczyk, S., Bindschadler, R. A., & Price, S. F. (2002). Changes in West Antarctic ice stream velocities: Observations and analysis. *Journal of Geophysical Research*, *107*(B11). doi:10.1029/2001JB001029.

Kääb, A. (2002). Monitoring high-mountain terrain deformation from air- and spaceborne optical data: Examples using digital aerial imagery and ASTER data. *ISPRS Journal of Photogrammetry and Remote Sensing*, *57*(1-2), 39–52.

Kääb, A. (2005). Combination of SRTM3 and repeat ASTER data for deriving alpine glacier flow velocities in the Bhutan Himalaya. *Remote Sensing of Environment*, *94*(4), 463–474.

Kääb, A., Huggel, C., Paul, F., Wessels, R., Raup, B., & Kieffer, H., et al. (2003a). Glacier monitoring from ASTER imagery: Accuracy and applications. *EARSel Proceedings*, *2*, 43–53.

Kääb, A., Lefauconnier, B., Melvold, K. (in press). Flow field of Kronebreen, Svalbard, using repeated Landsat7 and ASTER data. *Annals of Glaciology*, 42.

Kääb, A., Paul, F., Maisch, M., Hoelzle, M., & Haeberli, W. (2002). The new remote sensing derived Swiss glacier inventory: II. First results. *Annals of Glaciology*, *34*, 362–366.

Kääb, A., Reynolds, J. M., & Haeberli, W. (2005). Glacier and permafrost hazards in high mountains. In U. M. Huber, H. K. M. Bugmann, & M. A. Reasoner (Eds.), Global change and mountain regions (A state of knowledge overview). *Advances in global change research* (pp. 225–234). Dordrecht: Springer.

Kääb, A., Wessels, R., Haeberli, W., Huggel, C., Kargel, J., & Khalsa, S. J. S. (2003b). Rapid ASTER imaging facilitates timely assessment of glacier hazards and disasters. *EOS Transactions, American Geophysical Union*, *84*(13), 117–121.

Kadota, T., Seko, K., Aoki, T., Shujiwata, & Yamaguchi, S. (2000). Shrinkage of the Khumbu Glacier, east Nepal, from 1978 to 1995. In M. Nakawo, C. F. Raymond, & A. Fountain (Eds.), Debris-covered glaciers. *IAHS Publ.*, *vol. 264* (pp. 235–243).

Kamb, W. B. (1991). Rheological nonlinearity and flow instability in the deforming bed mechanism of ice stream motion. *Journal of Geophysical Research*, *96*, 16,585–16,595.

Kaser, G., Ames, A., & Zamora, M. (1990). Glacier fluctuations and climate in the Cordillera Blanca, Peru. *Annals of Glaciology*, *14*, 136–140.

Khromova, T. E., Dyurgerov, M. B., & Barry, R. G. (2003). Late-twentieth century changes in glacier extent in the Ak-shirak Range, central Asia, determined from historical data and ASTER imagery. *Geophyical Research Letters*, *30*(16), 1863. doi:10.1029/2003GL017233.

Kieffer, H.H., et al. (2000). New eyes in the sky measure glaciers and ice sheets, *Eos, Trans., Amer. Geophys. Union*, v. 81, p. 265 and 270–271.

Kjollmoen, B., Andreassen, L.M., Engeset, R.V., Elvehoy, H., & Jackson, M. (2004). Glaciological investigations in Norway in 2003. Report Number 4 by the Norwegian Water Resources and Energy Directorate (NVE), 97 pages.

Krabill, W., Hanna, E., Huybrechts, P., Abdalati, W., Cappelen, J., & Csatho, V., et al. (2004). Greenland ice sheet: Increased coastal thinning. *Geophysical Research Letters*, *31*, L24402. doi:10.1029/2004GL021533.

Lalande, P., Herman, N.M., Zillhardt, J. (1974). Cartes climatiques de l'Afghanistan: Kaboul, L'Institut de Meteorologie, Publication no. 4, v. 1, text, 47 p., v. 2, maps.

Lucchitta, B. K., & Ferguson, H. M. (1986). Antarctica—Measuring glacier velocity from satellite images. *Science*, *234*(4780), 1105–1108.

MacCracken, M. C., Barron, E., Easterling, D., Felzer, B., & Karl, T. (2001). Chapter 1: Scenarios for climate variability and change. *Climate change impacts on the United States: The potential consequences of climate variability and change. Report for the U.S. Global Change Research Program* (pp. 13–71). Cambridge UK: Cambridge University Press.

MacGregor, K. R., Anderson, R. S., Anderson, S. P., & Waddington, E. D. (2000). Numerical simulations of glacial-valley longitudinal profile evolution. *Geology*, *28*, 1031–1034.

Mayewski, A., Pregent, G. P., Jeschke, A., & Ahmad, N. (1980). Himalayan and trans-Himalayan Glacier fluctuations and the south Asian monsoon record. *Arctic and Alpine Research*, *12*(2), 171–182.

Meier, M. F., & Bahr, D. B. (1996). Counting glaciers: Use of scaling methods to estimate the number and size distributiuon of the glaciers of the world. In S. C. Colbeck (Ed.), Glaciers, ice sheets and volcanoes. A tribute to Mark F. Meier. *US Army CRREL special report*, *Vol. 96-27* (pp. 89–94).

Micklin, Ph. (2004). The Aral Sea crisis. In Ph. J.C.J., P. O. Zavialov, & P. P. Micklin (Eds.), *Dying and dead seas: Climatic versus anthropic causes, NATO science series* (pp. 99–124). Boston: Kluwer Academic Publishers.

Miller, K. J. (1984). *The International Karakoram Project*, *vols. 1 and 2*. Cambridge, UK.

Molnar, P., & England, P. (1990). Late Cenozoic uplift of mountain ranges and global climate change: Chicken or egg? *Nature*, *346*, 29–34.

Montgomery, D. R. (2004). GIS in tectonic geomorphology and landscape evolution. In M. P. Bishop, & J. F. Shroder Jr. (Eds.), *Geographic information science and mountain geomorphology* (pp. 425–460).

Mool, P. K. (1995). Glacier lake outburst floods in Nepal. *Journal of Nepal Geological Society*, *11*, 273–280.

Morales, B. (1969). Las lagunas y glaciares de la Cordillera Blanca y su control. *Revista Peruana de Andinismo y Glaciologica*, *8*, 76–79.

Naito, N., Nakawo, M., Kadota, T., & Raymond, C. F. (2000). Numerical simulation of recent shrinkage of Khumbu Glacier, Nepal Himalayas. In M. Nakawo, C. F. Raymond, & A. Fountain (Eds.), *Debris-covered glaciers, IAHS Publ.*, *vol. 264* (pp. 245–254).

Oerlemans, J. (1994). Quantifying global warming from the retreat of glaciers. *Science*, *264*, 243–245.

Oerlemans, J. (2005). Extracting a climate signal from 169 glacier records. *Science*, *308*, 675–677.

Ommanney, C. S. L. (1980). The inventory of Canadian glaciers: Procedures, techniques, progress and applications. *IAHS-AISH*, *126*, 35–44.

Oppenheimer, M. (1998). Global warming and the stability of the west Antarctic ice sheet. *Nature*, *393*, 325–332.

Paul, F. (2002). Changes in glacier area in Tyrol, Austria, between 1969 and 1992 derived from Landsat 5 TM and Austrian Glacier Inventory data. *International Journal of Remote Sensing*, *23*(4), 787–799.

Paul, F., Huggel, C., & Kääb, A. (2004). Mapping of debris-covered glaciers using multispectral and DEM classification techniques. *Remote Sensing of Environment*, *89*(4), 510–518.

Paul, F., Huggel, C., Kääb, A., & Kellenberger, T. (2003). Comparison of TM-derived glacier areas with higher resolution data sets. EARSeL workshop on remote sensing of land ice and snow, Bern, 11.-13.3.2002. *EARSeL eProceedings*, *vol. 2* (pp. 15–21).

Paul, F., & Kääb, A. (in press). Challenges for glacier inventorying from multispectral satellite data in the Canadian Arctic: Cumberland Peninsula, Baffin Island. *Annals of Glaciology*, 42.

Paul, F., Kääb, A., Maisch, M., Kellenberger, T., & Haeberli, W. (2002). The new remote-sensing-derived Swiss glacier inventory: I. Methods. *Annals of Glaciology*, *34*, 355–361.

Paul, F., Kääb, A., Maisch, M., Kellenberger, T., & Haeberli, W. (in press). Rapid disintegration of Alpine glaciers observed with satellite data. *Geophysical Research Letters*, *31*, L21402.

Pelto, M. S., & Hedlund, C. (2001). Terminus behavior and response time of North Cascade glaciers, Washington, U.S.A. *Journal of Glaciology*, *47*, 497–506.

Phillips, W. M., Sloan, V. F., Shroder, J. F., Sharma, P., Clarke, M. L., & Rendell, H. M. (2000). Asynchronous glaciation at Nanga Parbat, northwestern Himalaya Mountains, Pakistan. *Geology*, *28*(5), 431–434.

Rabus, B., Eineder, M., Roth, A., & Bamler, R. (2003). The Shuttle radar topography mission—A new class of digital elevation models acquired by spaceborne radar. *ISPRS Journal of Photogrammetry and Remote Sensing*, *57*, 241–262.

Rau, F., Mauz, F., De Angelis, H., Jaña, R., Arigony Neto, J., Skvarca, P., et al. (in press). Variations of glacier frontal positions on the Northern Antarctic Peninsula. *Annals of Glaciology*, *39*.

Raup, B., Kieffer, H., Hare, T., & Kargel, J. (2000). Generation of data acquisition requests for the ASTER satellite instrument for monitoring a globally distributed target. *IEEE Transactions on Geoscience and Remote Sensing*, *38*, 1105–1112.

Raup, B., Scharfen, G., Khalsa, S., & Kääb, A. (2001). The design of the GLIMS (Global Land Ice Measurements from Space) glacier database. *Eos Transactions Supplement, American Geophysical Society*, *82*(47).

Raymo, M. E., & Ruddiman, W. F. (1992). Tectonic forcing of the late Cenozoic climate. *Nature*, *359*, 117–122.

Reeh, N., Mohr, J. J., Madsen, S. N., Oerter, H., & Gundestrup, N. S. (2003). Three-dimensional surface velocities of Storstrømmen glacier, Greenland, derived from radar interferometry and ice-sounding radar measurements. *Journal of Glaciology*, 201–209.

Richardson, S. D., & Reynolds, J. M. (2000). Degradation of ice-cored moraine dams: Implications for hazard development. *International Association of Hydrological Sciences Publication*, *264*, 187–197.

Rignot, E., Braaten, D., Gogineni, S. P., Krabill, W., & McConnell, J. R. (2004). Rapid ice discharge from southeast Greenland glaciers. *Geophysical Research Letters*, *31*, L10401. doi:10.1029/2004GL019474.

Romanovsky, V. V. (2002). Water level variations and water balance of Lake Issyk-Kul. In J. Klerkx, & B. Imanackunov (Eds.), Lake Issyk-Kul: Its natural environment. *NATO Science Series* (pp. 45–58). Boston: Kluwer Academic Publishers.

Rott, H., Rack, W., Skvarca, P., & De Angelis, H. (2002). Northern Larsen ice shelf, Antarctica: Further retreat after collapse. *Annals of Glaciology*, *34*, 277–282.

Salzmann, N., Kääb, A., Huggel, C., & Algöwer, B. (2004). Assessment of the hazard potential of ice avalanches using remote sensing and GIS-modelling. *Norwegian Journal of Geography*, *58*, 74–84.

Scambos, T. A., Bohlander, J. A., Shuman, C. A., & Skvarca, P. (2004). Glacier acceleration and thinning after ice shelf collapse in the Larsen B embayment, Antarctica. *Geophysical Research Letters*, *31*, L18402. doi:10.1029/2004GL020670.

Scambos, T. A., Dutkiewicz, M. J., Wilson, J. C., & Bindschadler, R. A. (1992). Application of image cross-correlation to the measurement of glacier velocity using satellite image data. *Remote Sensing of Environment*, *42*(3), 177–186.

Scambos, T. A., Hulbe, C., Fahnestock, M. A., & Bohlander, J. (2000). The link between climate warming and break-up of ice-shelves in the Antarctic Peninsula. *Journal of Glaciology*, *46*(154), 516–530.

Searle, M. P. (1991). *Geology and tectonics of the Karakoram Mountains*. Wiley.

Shiyin, L., Wenxin, S., Yongping, S., & Gang, L. (2003). Glacier changes since the Little Ice Age maximum in the western Qilian Shan, northwest China, and consequences of glacier runoff for water supply. *Journal of Glaciology*, *49*, 117–124.

Shroder Jr., J. F. (1975). National Atlas of Afghanistan; a call for contribution. *Afghanistan Journal*, *Jg. 2*, 108–111.

Shroder Jr., J. F. (1978). Remote sensing of Afghanistan. *Afghanistan Journal*, *5*, 123–128.

Shroder Jr., J. F. (1983). The U.S.S.R. and Afghanistan Mineral Resources. In A. Agnew (Ed.), *International mineral resources a national perspective* (pp. 115–153). American Association for Advancement of Science.

Shroder Jr., J. F., & Bishop, M. P. (2000). Unroofing of the Nanga Parbat Himalaya. In M. A. Khan, P. J. Treloar, M. P. Searle, & M. Q. Jan (Eds.), Tectonics of the Nanga Parbat Syntaxis and the Western Himalaya. *Geological Society London, Special Publication*, *vol. 170* (pp. 163–179).

Shroder Jr., J. F., & Bishop, M. P. (in press-a). Glaciers of Afghanistan, In: *Satellite Image Atlas of Glaciers*, R. S. Williams Jr., & J. G. Ferrigno (Eds.). U.S. Geological Survey, Professional Paper 1386-F.

Shroder Jr., J. F., & Bishop, M. P. (in press-b). Glaciers of Pakistan, In: *Satellite Image Atlas of Glaciers*, R. S. Williams Jr., & J. G. Ferrigno (Eds.). U.S. Geological Survey, Professional Paper 1386-F.

Shroder Jr., J. F., & Giardino, J. R. (1978). Progress on rock glacier research. *Transactions of the Nebraska Academy of Sciences*, *vi*, 51–54.

Skvarca, P., Raup, B., & De Angelis, H. (2003). Recent behaviour of Glaciar Upsala, a fast-flowing calving glacier in Lago Argentino, southern Patagonia. *Annals of Glaciology*, *36*, 184–188.

Skvarca, P., Rott, H., & Nagler, T. (1995). Satellite imagery, a base line for glacier variation study on James Ross Island, Antarctica. *Annals of Glaciology*, *21*, 291–296.

Spikes, V. B., Csathó, B. M., Hamilton, G. S., & Whillans, I. M. (2003). Thickness changes on Whillans Ice Stream and Ice Stream C, West Antarctica, derived from laser altimeter measurements. *Journal of Glaciology*, *49*, 223–230.

Stafford, J. M., Wendler, G., & Curtis, J. (2000). Temperature and precipitation of Alaska: 50 year trend analysis. *Theoretical and Applied Climatology*, *67*, 33–44.

Stainforth, D. A., et al. (2005). Uncertainty in predictions of the climate response to rising levels of greenhouse gases. *Nature*, *433*, 403–406.

Stearns, L. A., & Hamilton, G. S. (in press). A new velocity map for Byrd Glacier, East Antarctica, from sequential ASTER satellite imagery. *Annals of Glaciology*, *41*.

Stearns, L. A., Hamilton, G. S., & Reeh, N. (in press). Multi-decadal record of ice dynamics of Daugaard Jensen Gletscher, East Antarctica, from satellite imagery and terrestrial field measurements. *Annals of Glaciology*, *42*.

Taschner, S., & Ranzi, R. (2002). Landsat-TM and ASTER data for monitoring a debris covered glacier in the Italian Alps within the GLIMS project. *Proceedings IGARSS 2002*(4), 1044–1046.

Tomkin, J. H., & Braun, J. (2002). The influence of alpine glaciation of the relief of tectonically active mountain belts. *American Journal of Science*, *302*, 169–190.

Wang, W. L., & Warner, R. C. (1998). Simulation of the influence of ice rheology on velocity profiles and ice-sheet mass balance. *Annals of Glaciology*, *27*, 194–200.

Warrick, R. A., Provost, C. L., Meier, M. F., Oerlemans, J., & Woodworth, P. L. (1996). Changes in sea level. In J. T. Houghton, L. G. Meira Filho, B. A. Calander, N. Harris, A. Kattenburg, & K. Maskell (Eds.), *Climate change 1995: The science of climate change* (pp. 359–405). Cambridge: Cambridge University Press.

Wessels, R., Kargel, J. S., & Kieffer, H. H. (2002). ASTER measurement of supraglacial lakes in the Mount Everest region of the Himalaya. *Annals of Glaciology*, *34*, 399–408.

Williams Jr., R.S., & Ferrigno, J.G. (Eds.) (2002). Glaciers of North America (volume J) and other volumes in the series Satellite Image Atlas of Glaciers of the World, U.S. Geol. Survey Prof. Pap. 1386-J, pp 405, and other volumes in Prof. Pap. 1386, U.S. Government Printing Office, Washington, D.C.

Williams Jr., R.S., Ferrigno, J.G., et al. (2006, estimated publication). Introduction (volume A) to series, Satellite Image Atlas of the Glaciers of the World, U.S. Geological Survey Professional Paper 1386-A (State of the Earth's Cryosphere at the Beginning of the 21st Century: Glaciers, Snow Cover, Floating Ice, and Permafrost).

Xiangsong, Z. (1992). Investigation of glacier bursts of the Yarkant River in Xinjiang, China. *Annals of Glaciology*, *16*, 135–139.

Xu, D., & Feng, Q. (1989). Characteristics of dangerous glacier lakes and their outburst, Tibet, Himalaya mountain. *Acta Geographica Sinica*, *44*(4), 343–345.

Yamada, T., & Motoyama, H. (1988). Contribution of glacier meltwater to runoff in glacierized watersheds in the Langtang Valley, Nepal Himalayas. *Bulletin of Glacier Research*, *6*, 65–74.

Yamada, T., & Sharma, C. K. (1993). Glacier lakes and outburst floods in the Nepal Himalaya. *International Association of Hydrological Sciences Publication*, *218*, 319–330.

Yang, Z., & Hu, X. (1992). Study of glacier meltwater resources in China. In R. L. Hooke (Ed.), Symposium on mountain glaciology Lanzhou, Gansu Province, China, 26–30 August 1991. *Proceedings. Annals of glaciology*, *vol. 16* (pp. 141–145).